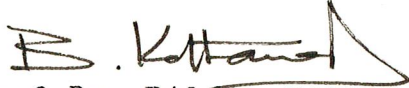SWITCHING TRANSIENTS

IN

UNDERGROUND POWER CABLES

A MASTER'S THESIS

in

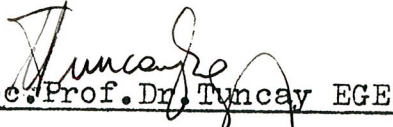Electrical Engineering

Middle East Technical University

By

H. Nebi ŞAHİN

May,1986

Approval of the Graduate School of Natural and Applied Sciences

Prof.Dr. Bilgin KAFTANOĞLU
Director

I certify that this thesis satisfies all the requirements as a thesis for the degree of Master of Science in Electrical Engineering
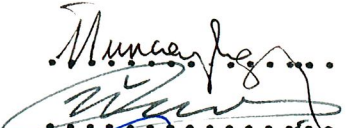
Assoc.Prof.Dr. Tuncay EGE
Chairman of the Department

We certify that we have read this thesis and that in our opinion it is fully adequate, in scope and quality, as a thesis for the degree of Master of Science in Electrical Engineering

Asst.Prof.Dr. Uğur ÜNVER
Supervisor

Examining Committee in Charge :

1. Assoc.Prof.Dr. Tuncay EGE (Chairman)
2. Asst.Prof.Dr. Uğur ÜNVER
3. Assoc.Prof.Dr. Mazhar ÜNSAL
4. Asst.Prof.Dr. Müzeyyen SARITAŞ

ABSTRACT

SWITCHING TRANSIENTS

IN

UNDERGROUND POWER CABLES

Şahin,H.Nebi

M.S. in Electrical Engineering

Supervisor : Asst.Prof.Dr.Uğur ÜNVER

1986

In this thesis, transient overvoltages due to cir -
cuit breaker operations in underground power cables are
investigated. Special attention is given to the sequen -
tial switching transients in cross- bonded cables.

Solution method combined the use of the modified
Fourier transform and the modal analysis.

The method of solution takes into account frequency
dependence of series impedance and shunt admittance
parameters. The effects of various system parameters, such
as, cable length, source impedance, shunt compensation
and pole closure angles on the transient performance of
the underground cable systems are investigated.

Key Words : Switching transient, modified Fourier
            transform, Modal analysis, Cross - bonded cable

ÖZET

YERALTI ENERJİ KABLOLARINDA MEYDANA GELEN

MANEVRA AŞIRI GERİLİMLERİ

ŞAHİN, H.Nebi

Yüksek Lisans Tezi, Elektrik Mühendisliği Bölümü

Tez Yöneticisi : Yrd.Doç.Dr. Uğur ÜNVER

1986

Bu tezde, yeraltı enerji kablolarına bir uçtan enerji verildiği sırada meydana gelen aşırı gerilimler incelenmiştir. Özellikle kesici kutuplarının farklı zamanlarda kapanması sonucu, kılıfı çapraz bağlı kablolarda meydana gelen aşırı gerilimler üzerinde durulmuştur.

Çözüm metodu olarak tadil edilmiş Fourier transform metodu modal analiz ile birlikte kullanılmıştır.

Çözüm metodu, sistemin frekansa bağlı seri empedans ve şönt admitans parametrelerini gözönüne almaktadır. Kablo uzunluğu, kaynak empedansı, kompanzasyon reaktörleri ve kapama anındaki faz açısı gibi değişik sistem parametrelerinin kabloda meydana gelen aşırı gerilimi nasıl etkilediği incelenmiştir.

Anahtar Kelimeler : Manevra aşırı gerilimi, tadil edilmiş
                    Fourier transform, Modal analiz,
                    Çapraz-bağlı kablo

ACKNOWLEDGEMENTS

TABLE OF CONTENTS

LIST OF TABLES

LIST OF FIGURES

NOMENCLATURE

A, B, C, D	:	Two-port admittance matrix parameters
E_{si}	:	Source voltage
f	:	Supply frequency
f_o	:	Fundamental frequency which is related to the observation time
G	:	Conductance of sheath earthing resistor, i.e. $G = \dfrac{1}{R_g}$
$\underset{\sim}{I}_i$	:	Column matrix of the currents at position i
$\underset{\sim}{I}_S, \underset{\sim}{I}_R$	:	Sending-end and receiving-end current column matrices, respectively. (Double suffix notation is used to denote individual phases)
i	:	Instantaneous current
L_s	:	Source inductance
l	:	Length of a transmission system
l_m	:	Cross-bonded cable major section length
N	:	Maximum number of the odd frequency harmonics
P	:	The matrix product. ZY
P_t	:	Transpose of P
Q	:	Voltage eigenvector matrix
R_g, R_e	:	Cable sheath earthing-resistors
T_o	:	Observation time or time interval
t	:	time
U	:	Unit matrix
u	:	Unit step function
V_m	:	Peak voltage
$\underset{\sim}{V}_i$	:	Column matrix of the phase voltages at position i. (Double suffix notation is used to denote individual phases) .

$\underset{\sim}{V}_x$	:	Intermediate voltage column matrix
$\underset{\sim}{V}_S, \underset{\sim}{V}_R$	:	Sending-end and receiving-end voltage column matrices, respectively
$\underset{\sim}{V}^{(m)}$	:	Modal voltage vector
v	:	Instantaneous voltage
v_{si}	:	Instantaneous source voltage
X_S	:	Source reactance
Y_R	:	Receiving-end admittance matrix
Y_S	:	Sending-end admittance matrix
Y_{SS}	:	Source admittance matrix
Y_s	:	Source admittance
Z, Y	:	Series impedance and shunt admittance matrices per unit length
Z_o, Y_o	:	Characteristic impedance and admittance matrices, respectively
Z_s	:	Source impedance
α	:	Shift constant or attenuation constant
Λ	:	Eigenvalue matrix of ZY
γ	:	Diagonal propagation constant matrix ; $\gamma = \Lambda^{\frac{1}{2}}$
ϵ	:	Permittivity
ϵ_0	:	Permittivity of free space
Ω	:	Truncation frequency
μ	:	Permeability
μ_0	:	Permeability of free space
ψ	:	Propagation coefficient matrix per unit length ; $\psi = P^{\frac{1}{2}}$
ρ	:	Resistivity
θ	:	Angular displacement of supply voltage
σ	:	Sigma factor

w :   Complex angular frequency

w_0 :   Fundamental angular frequency

w_s :   Supply angular frequency ; $w_s = 2\pi f$

CHAPTER 1

INTRODUCTION

1.1 General

For the reliable operation of power system networks
the maximum voltages appeared within the system have to
be determined. If the calculations and determinations of
the maximum transient overvoltages can be done at design
stage, precautions can be taken either to avoid the over-
voltages or to minimize their effects. The system
insulation level is also chosen according to the maximum
overvoltages appearing within the system. Insulation
level should be sufficiently high to withstand to the
maximum overvoltages developed in the system. Besides
that, there are strong economic reasons to keep the
insulation level as low as possible.

If the power system is subjected to sudden distur-
bances, transient overvoltages are induced in the con -
ductors. Sudden changes in voltage and current may be
the result of a lightning stroke, a fault or switching

of a part of the system. Effect of lightning on magnitude
of overvoltages decreases as the operating voltage level
increases. However, switching overvoltages are directly
related to the system voltages. As the system voltage
increases, switching overvoltage also increases.

Although a number of methods for calculating
switching transients exist, some are more accurate than
the others. The traditional method was the use of tran-
sient network analyser (TNA) type of analog computer.

1

This method provides facilities for forming a scale model
of the system being studied, using lumped values of
inductance, capacitance and resistance. The other method
called by Bewley Lattice diagram method is a form of the
travelling wave methods. The voltage existing at any
point on the line at time t may be obtained by using
the travelling waves which have arrived at the point prior
to time t, using reflection and refraction coefficients
in the lattice diagram method $\begin{bmatrix} 1 \end{bmatrix}$.

One of the most important factor in the choice of
calculation method is the frequency dependence of the
power system parameters. When a switching operation
takes place, the elements of a power system are subjected
to a wide range of frequencies from 50 Hz to the region
of 100 kHz $\begin{bmatrix} 1 \end{bmatrix}$. Over such a wide range, the values of
system parameters are not constant, but vary with frequency.
Therefore the calculation method should be capable of
representing both lumped and distributed parameters.

The Fourier transform method overcomes the difficulties
by deriving the time response from a transformation of
frequency spectrum of the network since calculations are
carried out in frequency domain in this method. This permits
the direct computation over any time interval for the points
of interest on the network.

The spreading of urban areas, and the increasing power
demand within them lead to the use of relatively long
cable circuits operating at high voltage levels. Under
steady - state operating conditions, currents are induced
in underground cable sheaths. In order to reduce the induced
currents, sheaths are transposed at some points throughout
the cable. Discontinuities of sheaths result in sheath

2

overvoltages. Therefore both the core insulation and the
sheath insulation must be capable of withstanding
overvoltages induced in the core and sheath.

1.2 Review of The Previous Studies

Bickford and Doepel [2] presented two methods for
the calculation of switching transients. One method based
on a lumped parameter representation of the system with
the use of (TNA) type of analog computer and the second one
based on the lattice diagram solution of the transmission
line wave equations.

Steady state analysis of cable systems were carried
out by Adamson, Taha and Wedepohl [3] in detail. In their
study, sheath voltages and losses in both crossbonded and
solidly bonded systems were calculated at power frequencies.

Wedepohl and Wilcox [4] developed a mathematical
model suitable for the analysis of travelling wave pheno-
mana in underground power transmission systems. They took
into account frequency dependent characteristics of cable
parameters, using modified Fourier transform method in
conjunction with the theory of natural modes.

Wedepohl and Indulkar [5] presented a mathematical
model of a single major section of a non - homogeneous
crossbonded cable. They used the Fourier transform method
and obtained the transient response at any point along a
short crossbonded system. Computation time in this method
was found to be directly proportional to the number of major
sections in the system. Therefore this method was suggested
to be not suitable for long crossbonded cable systems.

Dang [6] developed a model to represent a long
crossbonded cable. He extended the rotation matrix method

3

presented by Indulkar [7] . In Dang's model, each minor
section was considered to be consisting of lumped param-
eters, so that, any major section would be approximated
by an equivalent homogeneous section. Hence, the problem
of the cascading a large number of such major sections
was found to be independent of the number of major sections
involved.

Wilcox and Lawler [8] presented a realistic mathemat-
ical model of a crossbonded cable system taking into account
skin effect in the conductors and metallic sheaths and
mutual coupling between individual cables. The method may
be applied both to the long and short cable systems.

Wedepohl and Indulkar [9] developed a method for
computation of transient overvoltages in long crossbonded
cable systems utilizing Fourier Transform techniques. In
this method, by the application of the chain matrix theory
to the crossbonded cable systems, the amount of computa-
tional labor becomes independent of the number of major
sections. The component sub - matrices of the chain
matrix are obtained from the admittance sub - matrices.

Nagaoka and Ametani [10] calculated the transient
overvoltages on a crossbonded cable and compared the cal-
culated results with the field test results. They also
presented accurate and approximate methods of calculating
transients on a crossbonded cable. In their study, the
approximate method of calculation shows satisfactory
results with much smaller computation time if the number
of major sections is large.

1.3 Scope of the Present Work

As far as the switching transient studies are con -
cerned, previous studies are mainly devoted to single phase
energisation or three phase simultaneous energisation
of cable systems. However, in practice, the exact
simultaneous energisation, i.e. all the breaker poles
closing simultaneously is impossible due to the time
delays in closing or prearcing conditions.

The studies related to sequential switching
overvoltages in underground power cables using modified
Fourier transform method are not mentioned in the litera-
ture.

In the present work, switching transients in under-
ground power cables are studied using the modified
Fourier transform method in conjunction with the theory
of natural modes. The method has been verified to be quite
suitable for the solution of sequential switching trans -
ients in underground power cables. Effects of cable length,
source impedance, shunt compensation and pole closure
angles on the switching overvoltages are studied.

STEADY STATE ANALYSIS OF CABLE SYSTEMS

In order to study transient overvoltages by the modified Fourier transform method, the steady state solutions of voltages and currents are required.

The steady state solution described in the following sections is based on the modal analysis. A complete steady state solution may be obtained from the nodal matrix equations by making use of the boundary conditions.

2.1 Multiconductor Equations

The transmission equations for a homogeneous multiconductor system are generally given in the form;

$$\frac{\partial v(x,t)}{\partial x} = z(x) \cdot i(x,t) \qquad (2.1)$$

$$\frac{\partial i(x,t)}{\partial x} = y(x) \cdot v(x,t) \qquad (2.2)$$

The solutions of the above equations give the voltage vector $v(x,t)$ and the current vector $i(x,t)$ at any position x at time t. $z(x)$ and $y(x)$ are the series impedance and shunt admittance matrices per unit length, respect - ively.

Transforming equations (2.1) and (2.2) into frequency domain gives

$$\frac{dV}{dx} = -Z I \qquad (2.3)$$

$$\frac{d\underset{\sim}{I}}{dx} = - Y \underset{\sim}{V} \tag{2.4}$$

where $\underset{\sim}{V}$ and $\underset{\sim}{I}$ are vectors of dimension n, representing the voltages and currents at a distance x along the cable system containing n metallic conductors. Z and Y are system series impedance and shunt admittance matrices of dimensions nxn.

Differentian of equations (2.3) and (2.4) with respect to x yields

$$\frac{d^2\underset{\sim}{V}}{dx^2} = Z Y \underset{\sim}{V} \tag{2.5}$$

$$\frac{d^2\underset{\sim}{I}}{dx^2} = Y Z \underset{\sim}{I} \tag{2.6}$$

So, system voltage and current steady state equations are expressed as

$$\frac{d^2\underset{\sim}{V}}{dx^2} = P \underset{\sim}{V} \tag{2.7}$$

$$\frac{d^2\underset{\sim}{I}}{dx^2} = P_t \underset{\sim}{I} \tag{2.8}$$

where $\qquad P = Z Y \tag{2.9}$

$$P_t = Y Z \tag{2.10}$$

It is difficult to solve the multiphase problems because of the second order rates of change of voltage and current in each phase.

The modal method is based on a linear transformation of voltage and subsequent manipulations, so that second order differential relations only involve the diagonal matrices. Hence, the solutions of the differential equations can easily be carried out.

By means of a linear transformation, the actual voltage matrix $\underset{\sim}{V}$ is transformed to modal voltage vector $\underset{\sim}{V}^{(m)}$

$$\underset{\sim}{V} = Q \; \underset{\sim}{V}^{(m)} \tag{2.11}$$

Substituting equation (2.11) in equation (2.7) yields

$$Q \; \frac{d^2 \; \underset{\sim}{V}^{(m)}}{d \; x^2} = P \; Q \; \underset{\sim}{V}^{(m)} \tag{2.12}$$

rearranging

$$\frac{d^2 \; \underset{\sim}{V}^{(m)}}{d \; x^2} = Q^{-1} \; P \; Q \; \underset{\sim}{V}^{(m)} \tag{2.13}$$

If the transformation matrix (Q) is chosen in such a way that $Q^{-1} \; P \; Q$ is a diagonal matrix, i.e,

$$Q^{-1} \; P \; Q = \Lambda \tag{2.14}$$

where

$$\Lambda = \begin{bmatrix} \lambda_1 & 0 & \cdots & 0 \\ 0 & \lambda_2 & & \\ \vdots & & \ddots & \\ \vdots & & & \\ 0 & & & \lambda_n \end{bmatrix}_{n \times n} \qquad (2.15)$$

and λ_1, λ_2, ... λ_n are eigenvalues of the matrix P.

Transforming the matrix P into a diagonal form is a well known process in matrix theory. The transformation matrix Q is formed from the eigenvectors corresponding to each eigenvalue of the characteristic equation of matrix P. The dimension of the transformation matrix Q is (nxn) and it is nonsingular.

Equation (2.13) may be written in matrix form as;

$$\frac{d^2}{dx^2} \begin{bmatrix} V_1^{(m)} \\ V_2^{(m)} \\ \vdots \\ V_n^{(m)} \end{bmatrix} = \begin{bmatrix} \lambda_1 & 0 & \cdots & 0 \\ 0 & \lambda_2 & & \\ \vdots & & \ddots & \\ 0 & & & \lambda_n \end{bmatrix} \begin{bmatrix} V_1^{(m)} \\ V_2^{(m)} \\ \vdots \\ V_n^{(m)} \end{bmatrix} \qquad (2.16)$$

where $V_n^{(m)}$ is the nth conductor modal voltage.

9

For the ith mode,

$$\frac{d^2}{dx^2} V_i^{(m)} = \lambda_i V_i^{(m)} \qquad i=1,\ldots.n \qquad (2.17)$$

Defining

$$\gamma_i = \lambda_i^{1/2} = \alpha + j\beta$$

where λ_i : the ith element of the diagonal matrix

γ_i : the propagation constant for the ith mode

α : the attenuation constant of the ith mode

β : the velocity factor of the ith mode

The velocity, of the ith mode, $v = 2\pi f / \beta$

The solution of equation (2.17) for the ith element has the form;

$$V_i^{(m)} (x) = \exp (-\gamma_i x) k_1 + \exp (\gamma_i x) k_2 \qquad (2.18)$$

where x is the distance measured from sending-end, k_1 and k_2 are arbitrary scalar constants.

Since there are n values for λ_i, there exist n modes and the total solution includes n such equations which may be written in matrix form as

$$\underset{\sim}{V}^{(m)} = \exp (-\gamma x) K_1 + \exp (\gamma x) K_2 \qquad (2.19)$$

where K_1 and K_2 are arbitrary column matrices of order n and exp $(\mp \gamma x)$ are diagonal matrices.

To turn back to the phase quantities, equation (2.11) is used again, in matrix notation

10

$$\underset{\sim}{V}(x) = Q \exp(-\gamma x) \, Q^{-1} \, \underset{\sim}{V}_i + Q \exp(\gamma x) Q^{-1} \underset{\sim}{V}_r \quad (2.20)$$

where $\underset{\sim}{V}_i$ and $\underset{\sim}{V}_r$ are column matrices of incident and reflected waves. If we define a matrix ψ, such as

$$\psi = Q \, \gamma \, Q^{-1} \quad\quad\quad (2.21)$$

then, the equation (2.20) can be written in the following form;

$$\underset{\sim}{V}(x) = \exp(-\psi x) \, \underset{\sim}{V}_i + \exp(\psi x) \, \underset{\sim}{V}_r \quad\quad (2.22)$$

The solution of the system steady state currents can be readily obtained from equation (2.22) by using the system first order differential equation,

$$\underset{\sim}{I} = -Z^{-1} \frac{d\underset{\sim}{V}}{dX} \quad\quad\quad (2.23)$$

So that, matrix notation of the system steady state currents takes the form ;

$$\underset{\sim}{I} = Y_o \left[\exp(-\psi x) \, \underset{\sim}{V}_i - \exp(\psi x) \, \underset{\sim}{V}_r \right] \quad\quad (2.24)$$

where $\quad Y_o = Z^{-1} \psi \quad\quad\quad\quad\quad (2.25)$

Y_o is identified as characteristic admittance ma - trix of the transmission system.

Incident and reflected wave column matrices, $\underset{\sim}{V}_i$ and $\underset{\sim}{V}_r$ may be eliminated from the equations (2.22) and (2.24) by applying boundary conditions.

11

2.2 Application of Boundary Conditions

The relationship between the sending and receiving ends of a two-port network can be derived from equations (2.22) and (2.24). V_s and I_s are sending-end voltage and current vectors, respectively. Substituting V_s and I_s in equations (2.22) and (2.24) at $x = 0$, V_i and V_r may be found as

$$V_i = \frac{1}{2} (V_s + Y_o^{-1} I_s)$$

$$V_r = \frac{1}{2} (V_s - Y_o^{-1} I_s) \tag{2.26}$$

where $Y_o^{-1} = Z_o$, characteristic impedance.

Substitution of equation (2.26) into equations (2.22) and (2.24) gives,

$$V_x = \frac{1}{2} (V_s + Z_o I_s) \exp (-\psi x) + \frac{1}{2} (V_s - Z_o I_s) \exp (\psi x)$$

$$\tag{2.27}$$

$$I_x = \frac{1}{2} (Y_o V_s + I_s) \exp (-\psi x) - \frac{1}{2} (Y_o V_s - I_s) \exp (\psi x)$$

If we substitute hyperbolic functions in place of exponential functions, the equations (2.27) give

$$I_s = Y_o \coth (\psi x) V_s - Y_o \operatorname{cosech} (\psi x) V_x$$

$$\tag{2.28}$$

$$I_x = - Y_o \operatorname{cosech} (\psi x) V_s + Y_o \coth (\psi x) V_x$$

If the receiving-end voltages and currents are concerned the system equations become

$$
\begin{bmatrix} I_S \\ I_R \end{bmatrix} = \begin{bmatrix} A & -B \\ -B & A \end{bmatrix} \begin{bmatrix} V_S \\ V_R \end{bmatrix} \tag{2.29}
$$

where $A = Y_o \coth(\psi 1)$

$B = Y_o \operatorname{cosech}(\psi 1)$

$Y_o = Y \, Q \, \gamma \, Q^{-1}$

Y_o and ψ are characteristic admittance and propagation coefficient matrices, respectively.

Equation (2.29) yields a complete steady state solution for the transmission system under consideration in terms of the underground cable basic constants.

The hyperbolic functions used in the two-port equation (2.29) are formulated in terms of exponentials to avoid overflow.

The orders of A and B matrices depend on the orders of series impedance matrix Z, and shunt admittance matrix Y of the transmission system.

Characteristic admittance matrix Y_o is expressed as

$$
Y_o = Y \psi^{-1} = Y \, Q \, \gamma^{-1} Q^{-1} \tag{2.30}
$$

where $\psi = P^{1/2} = (ZY)^{1/2}$

γ is a diagonal matrix, formed by the eigenvalues of ψ.

Substituting equation (2.30) into the nodal parameters in the equation (2.29) gives

13

$$A = Y_O \coth (\psi 1) = YQ\delta^{-1} \coth (\delta 1) . Q^{-1}$$

$$(2.31)$$

$$B = Y_O \cosech (\psi 1) = YQ\delta^{-1} \cosech(\delta 1) . Q^{-1}$$

Equation (2.31) is easily used to determine nodal parameters in the computer study.

If a three phase load with an impedance matrix Z_L is connected at the receiving-end, voltages and currents concerning Z_L may be written as

$$\underset{\sim}{I}_L = Z_L^{-1} \underset{\sim}{V}_R = Y_L \underset{\sim}{V}_R \qquad (2.32)$$

where Y_L is admittance matrix and $\underset{\sim}{I}_L$ is column vector representing the currents flowing through the impedance Z_L. If we combine equations (2.32) and (2.31), the system equation becomes,

$$\begin{bmatrix} \underset{\sim}{I}_S \\ \underset{\sim}{I}_R \end{bmatrix} = \begin{bmatrix} A & -B \\ -B & A+Y_L \end{bmatrix} \begin{bmatrix} \underset{\sim}{V}_S \\ \underset{\sim}{V}_R \end{bmatrix} \qquad (2.33)$$

2.3 Cross-Bonded Cable System

Most of the underground power cables used in high-voltage system are cross-bonded. In cross-bonded cable systems sheath currents under steady-state operating conditions are reduced by transposing the sheaths at joint points. Such a cable system is made up of a num - ber of major sections each of which comprises three minor sections as shown in Fig.2.1.

14

c : core
s : sheath

sheath
earthing
resistance
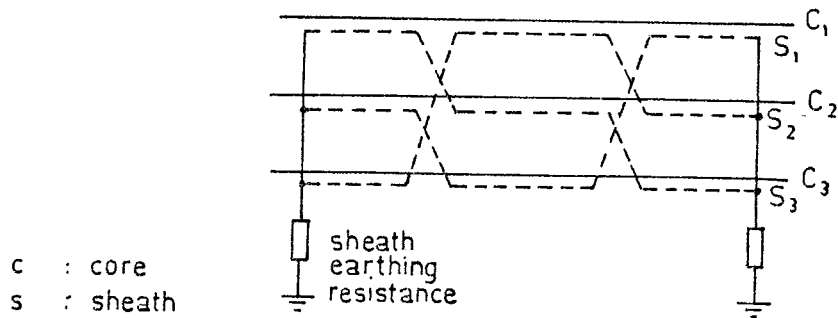
Fig.2.1 Major section of a cross-bonded cable.

The series impedance and shunt admittance matrices for each minor section are evaluated from the parameters of the systems, as shown in Appendix A.

For a crossbonded cable containing any number of major sections, series impedance and shunt admittance matrices have been formed using Dang's approach [6] which takes the advantage of the fact that minor section lenghts are electrically short as far as the observation time is concerned. That is, the length of a minor section is much shorter than the wavelength of the highest harmonic component used in representing a transient wave along a cross-bonded cable. Hence each minor section can be represented by lumped parameter networks and each major section can be approximated by an equivalent homogeneous section which is formed by compounding three such minor sections. Dang shows that, the problem of cascading a large number of such major sections is then independent of the number of sections

15

involved. The method is relatively simple to compute, and results in a considerable saving in computer time due to the fact that all but two of the eigenvalues of the homogeneous matrix product ZY can be obtained by inspection, the remaining two being the roots of a simply derived quadratic equation.

According to the sheath earthing conditions two-port nodal matrix equation of a crossbonded cable system is obtained.

2.3.1 Sheaths Earthed Through Resistors

If the sheath earthing resistors used at major sections ends, system becomes nonhomogeneous even though each major section is homogeneous. If the sheath earthing resistor R is represented by two parallel connected resistors, both ends of the major sections will have two resistors with the resistance 2R or conductance G/2, as illustrated in Fig.2.2.
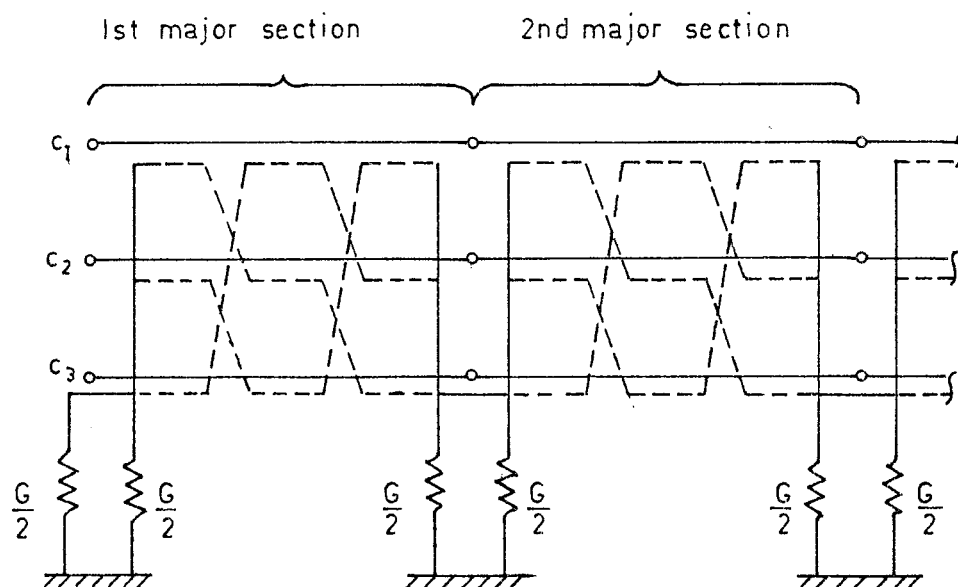
Fig.2.2   Representation of two adjacent major sections

16

Thus, all the system consists of n homogeneous major sections which can be compounded to form a two-port matrix equation of the system.

Since cable sheaths are solidly interconnected at the ends of each major section, three sheaths can be reduced to a single one. Hence, series impedance and shunt admittance matrices of the system have orders of 4x4, consequently the order of A and B matrices also becomes 4x4, as can be seen in Appendix B.

Two-port matrix equation of each major section becomes

$$
\begin{bmatrix} I_1 \\ I_2 \end{bmatrix} = \begin{bmatrix} A + Y_G & -B \\ -B & A+Y_G \end{bmatrix} \begin{bmatrix} V_1 \\ V_2 \end{bmatrix} \tag{2.34}
$$

where

$$
Y_G = \begin{bmatrix} 0 & 0 & 0 & 0 \\ 0 & 0 & 0 & 0 \\ 0 & 0 & 0 & 0 \\ 0 & 0 & 0 & G/2 \end{bmatrix}
$$

Subscripts 1, and 2 refer to sending-end and receiving - end of a major section, respectively. Currents entering the major section at either end are considered as posi - tive. G is the contact conductance of sheath earthing resistor. Also, in equation (2.34)

17

$$A = Y_o \coth (\psi_m \, l_m)$$

$$B = Y_o \operatorname{cosech} (\psi_m \, l_m)$$

ψ_m, and l_m are propagation coefficient matrix and the length of the major section, respectively; Y_o is major section characteristic admittance matrix.

Two-port matrix equation of the cable system consisting of n major sections can be written as

$$\begin{bmatrix} I_S \\ I_R \end{bmatrix} = \begin{bmatrix} A_n + Y_G & -B_n \\ -B_n & A_n + Y_G \end{bmatrix} \begin{bmatrix} V_S \\ V_R \end{bmatrix} \qquad (2.35)$$

where

I_S, V_S, and I_R, V_R are sending and receiving ends column vectors of the cable system, A_n and B_n are square matrices of order 4 and given by

$$A_n = Y_o' \coth (n\psi_m' \, l_m)$$

$$B_n = Y_o' \operatorname{cosech} (n \, \psi_m' \, l_m)$$

where Y_o' and ψ_m' are modified characteristic admittance and propagation coefficient matrices which takes into account the sheat earthing resistors; n is the number of major sections [11].

2.3.2 Sheaths Solidly Earthed

A possible simplification that can be introduced is based on the assumption that the sheaths at the major section terminals are solidly earthed. This would cause the voltage of the equivalent sheath to be zero, so that,

18

the row and column corresponding to cable sheath may be
eliminated from matrix equations. The reduction of
series impedance and shunt admittance matrices of cable
is given in details in Appendix B.

Two-port matrix equation of each major section of
the system may now be written as

$$
\begin{bmatrix} I_1 \\ I_2 \end{bmatrix} = \begin{bmatrix} A & -B \\ -B & A \end{bmatrix} \begin{bmatrix} V_1 \\ V_2 \end{bmatrix}
\qquad (2.36)
$$

where I_1, V_1 and I_2, V_2 are sending-end and receiving-end
column vectors of a major section respectively,

$$
A = Y_o \ \text{coth} \ (\psi_m \ l_m)
$$

$$
B = Y_o \ \text{cosech} \ (\psi_m \ l_m)
$$

where, ψ_m : propagation coefficient matrix

Y_o : characteristic admittance matrix

l_m : major section length

If a cross-bonded cable system consists of n major
section, two-port matrix equation of the overall system
becomes

$$
\begin{bmatrix} I_S \\ I_R \end{bmatrix} = \begin{bmatrix} A_n & -B_n \\ -B_n & A_n \end{bmatrix} \begin{bmatrix} V_S \\ V_R \end{bmatrix}
\qquad (2.37)
$$

where A_n and B_n are matrices of order 3 and given by

19

$$A_n = Y_o \coth (n \, \psi_m \, l_m)$$

$$B_n = Y_o \operatorname{cosech} (n \, \psi_m \, l_m)$$

where, n is the number of major sections in cascade.

2.4 Mathematical Formulations of System Voltages

In the mathematical formulation of the system volt-
ages, sources are represented by their Norton equivalents
as shown in Fig.2.3.

2.4.1 Case 1 : Cable Sheaths Earthed Through Resistors

If the sheaths are earthed through resistors at the
ends of each major section, the impedance and admittance
matrices as well as the matrices A and B will have
orders of 4 x 4.

Assume a crossbonded cable system consisting of n
major sections. For the evaluation of intermediate volt-
ages, the overall cable is seperated into two homogeneous
parts, one having k major sections in cascade, and the
other having m major sections in cascade, the total
being n, as shown in Fig.2.4. In the figure, possible
connections of shunt reactors as well as the Norton
equivalent circuit of the source are also shown.

Consider an intermediate point x, at which voltage
and current vectors are V_x and I_x, respectively.
The injected current, I_x at x is zero. The nodal
equation of the cable neglecting the end terminations
may be written as
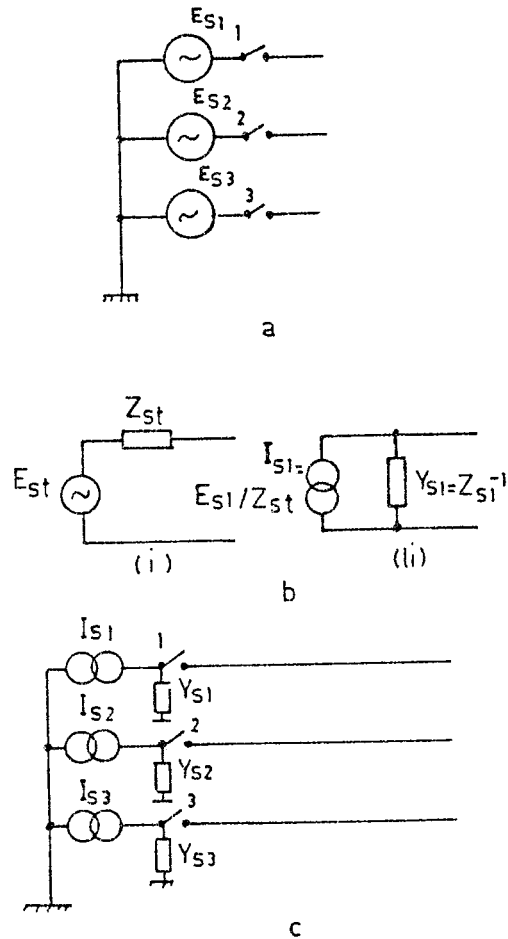
Fig.2.3   Representation of Source

    a) General representation of a source

    b)   Single-phase representation

         (i)   Thevenin equivalent of the source

         (ii) Norton equivalent of the source

    c)   Norton equivalent of the source
         (Three-phase representation)
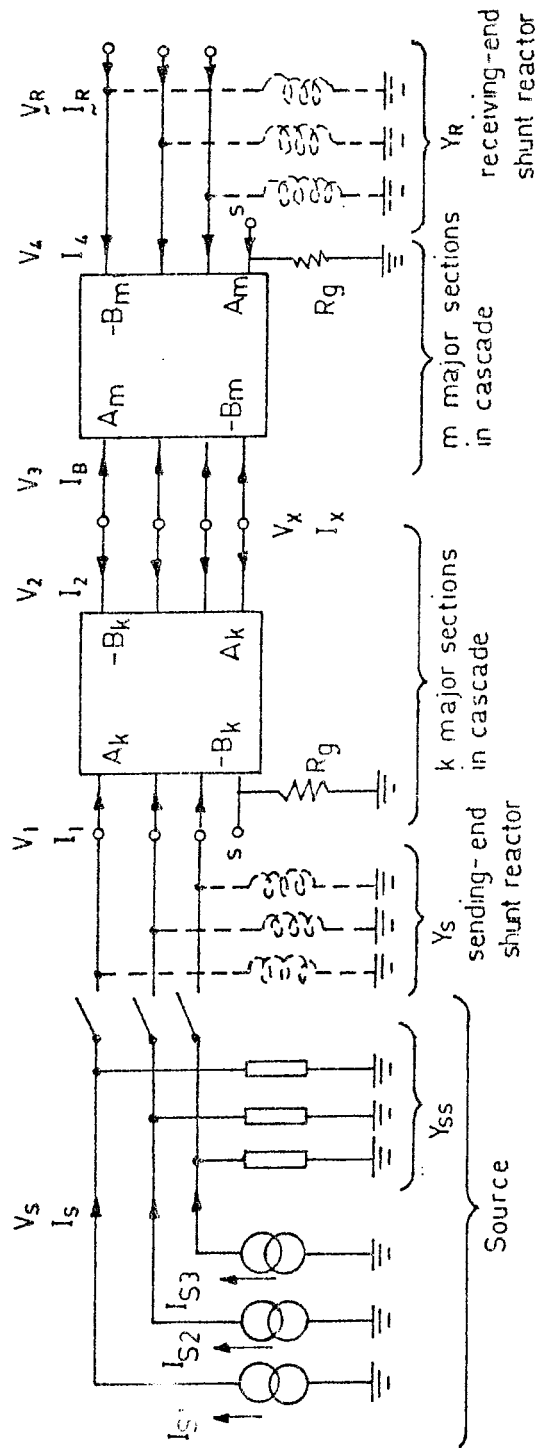
Fig.2.4 Equivalent circuit diagram of a crossbonded cable system,

sheaths are earthed through resistors.

$$
\begin{bmatrix} I_1 \\ 0 \\ I_4 \end{bmatrix} = \begin{bmatrix} A_k + Y_G & -B_k & 0 \\ -B_k & A_k + A_m & -B_m \\ 0 & -B_m & A_m + Y_G \end{bmatrix} \begin{bmatrix} V_1 \\ V_x \\ V_4 \end{bmatrix} \qquad (2.38)
$$

where
$$ A_k = Y_0' \; \coth \; (k \psi_m' l_m) $$
$$ A_m = Y_0' \; \coth \; (m \psi_m' l_m) $$
$$ B_k = Y_0' \; \mathrm{cosech} \; (k \psi_m' l_m) $$
$$ B_m = Y_0' \; \mathrm{cosech} \; (m \psi_m' l_m) $$

l_m = cable major section length

$V_x = V_2 = V_3$ = junction node voltage **vector**

V_1, V_4 and I_1, I_4 are as shown in **Fig.2.4.**

Y_G is the admittance matrix corresponding to the earthing resistance and is given by

$$
Y_G = \begin{bmatrix} 0 & 0 & 0 & 0 \\ 0 & 0 & 0 & 0 \\ 0 & 0 & 0 & 0 \\ 0 & 0 & 0 & 1/R_g \end{bmatrix}
$$

where $R_g = 2/G$ and is shown in Fig.2.4.

V_x in the nodal equation (2.38) may be expressed as

$$ V_x = (A_k + A_m)^{-1} (B_k V_1 + B_m V_4) \qquad (2.39) $$

where V_1 and V_4 are voltage vectors which are equal to the sending-end and receiving-end voltage vectors, V_s

23

and V_R respectively. Then, the intermediate voltage vector V_X is expressed in terms of the V_S and V_R.

When V_X is eliminated from equation (2.38), the nodal matrix equation of the cable shown in Fig.2.4 becomes

$$\begin{bmatrix} I_1 \\ I_4 \end{bmatrix} = \begin{bmatrix} A_n + Y_G & -B_n \\ -B_n & A_n + Y_G \end{bmatrix} \begin{bmatrix} V_1 \\ V_4 \end{bmatrix} \qquad (2.40)$$

where $A_n = Y_0' \coth (n \psi_m' l_m)$

$B_n = Y_0' \operatorname{cosech} (n \psi_m' l_m)$

Y_G is the same as in the equation (2.38)

n = total number of major sections

Including the admittance matrices of the shunt reactors and of the source, and taking the receiving-end currents to be zero, (receiving-end unterminated) equation (2.40) becomes,

$$\begin{bmatrix} I_S \\ 0 \end{bmatrix} = \begin{bmatrix} A_n + Y_G + Y_S + Y_{SS} & -B_n \\ -B_n & A_n + Y_G + Y_R \end{bmatrix} \begin{bmatrix} V_S \\ V_R \end{bmatrix} \qquad (2.41)$$

where V_S and V_R are sending-end and receiving-end voltage vectors of the order 4x1. I_S is the sending-end current vector of the order 4x1, in which the current corresponding to the sheath is zero. Y_S and Y_R are sending-end and receiving-end shunt reactor admittance matrices, respectively. Y_{SS} is the source admittance matrix. Y_S, Y_R and Y_{SS} are all

24

diagonal matrices of the order of 4x4. The last diagonal
elements corresponding to the sheath for the three of
these admittance matrices are all zero.

The voltage vectors $\underset{\sim}{V}_S$ and $\underset{\sim}{V}_R$ are obtained by solving the equation (2.41) as follows

$$\underset{\sim}{V}_S = (A - BD^{-1} B)^{-1} \underset{\sim}{I}_S \qquad (2.42)$$

$$\underset{\sim}{V}_R = D^{-1}B (A - BD^{-1} B)^{-1} \underset{\sim}{I}_S \qquad (2.43)$$

where $A = A_n + Y_G + Y_S + Y_{SS}$

$B = B_n$

$D = A_n + Y_G + Y_R$

and the intermediate voltage $\underset{\sim}{V}_X$ may be written as

$$\underset{\sim}{V}_X = (A_k + A_m)^{-1} (B_k \underset{\sim}{V}_S + B_m \underset{\sim}{V}_R) \qquad (2.44)$$

where A_k, A_m, B_k and B_m are the same as given in equation (2.38)

Thus, $\underset{\sim}{V}_S$ and $\underset{\sim}{V}_R$ are expressed in terms of the
sending-end current vector $\underset{\sim}{I}_S$. The intermediate voltage
$\underset{\sim}{V}_X$ is expressed in terms of the sending-end and receiving-end voltages.

2.4.2 Case 2 : Cable Sheaths Solidly Earthed

If the sheaths of the crossbonded cable are solidly
earthed at the both ends of each major section, series
impedance and shunt admittance matrices become square matrices
of order 3. Thus two port nodal parameters A and B will

have orders of 3x3. In this case, nodal matrix equation of the system has the same form as that of equation (2.41), and may be written as,

$$
\begin{bmatrix} I_S \\ \\ o \end{bmatrix} = \begin{bmatrix} A_n + Y_S + Y_{SS} & -B_n \\ \\ -B_n & A_n + Y_R \end{bmatrix} \begin{bmatrix} V_S \\ \\ V_R \end{bmatrix} \qquad (2.45)
$$

where I_S, V_S, and V_R are column vectors of order 3x1; A_n, and B_n are the square matrices of the order of 3x3 and are the same as given in equation (2.37). Y_S, Y_{SS}, and Y_R are the diagonal matrices of the order of 3x3.

Steady state response of the crossbonded cables, at sending-end, and receiving-end as well as at any point along the cable are obtained in a similar way as given by equations (2.42), (2.43) and (2.44), respectively. In this case, in the expression of intermediate voltage V_X, the nodal parameters are expressed as

$$
A_k = Y_o \coth (k \, \psi_m \, l_m)
$$

$$
A_m = Y_o \coth (m \, \psi_m \, l_m)
$$

$$
B_k = Y_o \cosech(k \, \psi_m l_m)
$$

$$
B_m = Y_o \cosech(m \, \psi_m l_m)
$$

Transient response of cable systems at sending-end, receiving-end and intermediate point are obtained making use of these equations while applying the modified Fourier transform method.

CHAPTER 3

TRANSIENT ANALYSIS OF CABLE SYSTEMS

When a switching operation takes place, the elements of the power system are subjected to voltages and currents having a wide range of frequencies. The frequency dependence of the parameters of the system can be accomodated by the use of methods based on the Fourier transform. Fundamentally, the method requires the calculation of the response of the system over a range of frequencies and the use of the inverse Fourier transform to transform the response from the frequency domain into the time domain. In the method of Fourier analysis, the waveform is split into an infinite number of frequencies differing from each other by an infinitesimal step length. However it is not possible to have an infinite number of frequencies and infinitesimal step length in numerical work. A finite step length is thus chosen with a finite upper frequency limit.

3.1 Modified Fourier Transform

After the steady-state response of the transmission system is formulated Fourier transform technique is used for the transient solution. The following is a summarised theory:

$$F(w) = \int_{-\infty}^{+\infty} f(t) \exp(-jwt) \, dt \qquad (3.1)$$

and

$$f(t) = \frac{1}{2\pi} \int_{-\infty-j\alpha}^{+\infty-j\alpha} F(w) \exp(jwt) \, dw \qquad (3.2)$$

In equations (3.1) and (3.2) f(t) is the time-dependent function, F(w) is the Fourier transform of it and α is a constant which is used to stabilize the integrand and, consequently to increase the computational efficiency of the numerical solution. In many cases, the poles of the transform F(w) lie close to the real axis. This causes the integrand to peak over a series of small intervals close to the poles. The integration is stabilized by choosing a line of integration displaced from the real axis by the shift factor α .

Defining a complex frequency $w = w' - j\alpha$, the inverse modified transform can be expressed by

$$f(t) = \frac{1}{2\pi} \int_{-\infty-j\alpha}^{+\infty-j\alpha} F(w'-j\alpha) \exp\left[j (w'-j\alpha)t \right] \, dw'$$

or

$$f(t) = \frac{\exp(\alpha t)}{2\pi} \int_{-\infty-j\alpha}^{+\infty-j\alpha} F(w'-j\alpha) \exp(jw't) \, dw' \qquad (3.3)$$

In a real physical system, the function f(t) is purely real and we have

$$\text{Real } F(w) = \text{Real } F(-w)$$
$$\text{Imag } F(w) = -\text{Imag } F(-w) \qquad (3.4)$$

giving the semi-infinite form of the Fourier Inversion integral as

$$f(t) = \frac{\exp(\alpha t)}{\pi} \, \text{Re} \int_{0}^{\infty-j\alpha} F(w'-j\alpha).\exp(jw't).\,dw' \qquad (3.5)$$

3.2 Numerical Form of the Modified Fourier Transform

Fourier Inversion integral (eqn.3.5) is evaluated by numerical methods in computer. For this purpose a finite frequency step length w_0 is required to define $w' = nw_0$.

Thus

$$f(t) = \frac{\exp(\alpha t)}{\pi} \, \text{Real}\left[\sum_{n=0}^{\infty} F(nw_0-j\alpha).\exp(jnw_0t).w_0\right] \qquad (3.6)$$

It is necessary to choose an upper limit frequency Ω, for the numerical integration. This frequency is called truncation frequency. Because of this finite upper limit for frequency harmonics, a certain amount of oscillations known as Gibb's Phenomena takes place.

Gibb's oscillations are reduced by introducing a weighting factor σ into the Fourier transform, i.e.

$$\sigma = \frac{\sin(\pi w/\Omega)}{(\pi w/\Omega)} \qquad (3.7)$$

However, it increases the rise time.

This factor decreases as the frequency increases. Therefore, it has little effect on low frequencies but damps out the higher frequencies.

The finite step length w_o causes the waveform to repeat at intervals $T = 2\pi/w_o$. If the parameters are calculated at mid-step length rather than on one side of the interval, the accuracy is increased for the same number of steps. If we take the step length $2w_o$, calcula - tion are performed at mid-steps $(2n-1)$ w_o. Thus, the transforms are calculated at the odd harmonics effectively. Then the numerical form may be expressed, using the trapezoidal rule as ;

$$f(t) = \frac{2w_o}{\pi} \exp(\alpha t) \, \text{Real} \left\{ \sum_{n=1}^{N} \sigma \cdot F \left[(2n-1)w_o - j\alpha \right] \cdot \exp \left[j(2n-1) \, w_o t \right] \right\}$$

$$(3.8)$$

where n is the number of odd frequency harmonics, N is the maximum number of odd frequency harmonics. In this case, frequency upper limit becomes $2N \cdot w_o$, and sigma factor is given by

$$\sigma = \frac{\sin \left[\pi (2n - 1) / 2N \right]}{\pi (2n - 1) / 2N} \qquad (3.9)$$

For the numerical solution, first of all observ - ation time T_o is chosen. Then the step length $2w_o$ and the shift factor α are determined accordingly.

The step length $2w_o$ causes the waveform to repeat at intervals · ·

$$T_o = 2\pi/2w_o = \pi/w_o = \frac{1}{2f_o}$$

The relation between the step length and the observation time is

$$T_o \leq \frac{\pi}{w_o}$$

Gibb's oscillations don't appear for $t \leq \frac{T_o}{2}$, hence the fundamental frequency f_o may be chosen to satisfy the relation

$$\frac{1}{4\,T_o} \leq f_o \leq \frac{1}{2\,T_o} \tag{3.10}$$

When a fundamental frequency is chosen to correspond to twice the observation time, $\alpha = 2w_o$ is quite adequate

The greater the truncation frequency used, the more accurate the response in time domain could be obtained. However, it causes more computation time. Therefore an optimum truncation frequency is to be chosen.

3.3 Three Phase Simultaneous Energisation

The closure of switch is simulated by the application, at the switch terminals, of a voltage equal and opposite to the existing voltage across the switch, before closure. The resultant voltage which appears across the switch after the closure, will be zero.

In general, the energisation voltages are sinusoidal

$$V_{si} = V_{max} \cos (w_s t + \theta_i + \phi_i) \, , \quad i = 1,2,3 \tag{3.11}$$

where θ_1, θ_2, θ_3 are the phase displacements of the supplied voltages being $0°$, $120°$, and $240°$ for a balanced three phase system. ϕ_1, ϕ_2, ϕ_3 are the pole closure angles, and w_s is the angular frequency of the supply voltage.

Fourier transform of these voltages will have the following form,

$$V_{si}(w) = V_m \cos(\theta_i + \phi_i) \cdot \frac{jw}{w_s^2 - w^2}$$

$$- V_m \sin(\theta_i + \phi_i) \frac{w_s}{w_s^2 - w^2} \qquad i = 1, 2, 3 \qquad (3.12)$$

For practical purposes infinite bus-bar source has been simulated by a voltage source behind a very small resistance of the order of 10^{-6} ohms. A generator is simulated by a voltage source behind an inductance or behind and inductance and resistance.

In calculations, Thevenin equivalent of the source representation is converted to Norton equivalent as in Fig. 2.3. In that case, the injected currents to the circuit breaker poles are;

$$\begin{bmatrix} I_{s1} \\ I_{s2} \\ I_{s3} \end{bmatrix} = \begin{bmatrix} Y_{s1} & 0 & 0 \\ 0 & Y_{s2} & 0 \\ 0 & 0 & Y_{s3} \end{bmatrix} \begin{bmatrix} E_{s1} \\ E_{s2} \\ E_{s3} \end{bmatrix} \qquad (3.13)$$

where I_{s1}, I_{s2} and I_{s3} are sending-end injected currents. Y_{s1}, Y_{s2} and Y_{s3} are the shunt admittances which correspond to the source impedances of of the first, second and the third phases, respectively. E_{s1}, E_{s2} and E_{s3} are the source voltages of each phase.

Sending-end currents are calculated at each frequency step using equation (3.13), and they are substituted in the steady-state equations (2.38), and (2.39) to find the sending-end and receiving-end voltages corresponding to the frequency considered. These calculations are repeated for each frequency step up to the truncation frequency with the chosen step length. After the frequency response of the system is obtained, time response is found using the numerical form of the inverse Fourier transform given by equation (3.8).

3.4 Three Phase Sequential Energisation

3.4.1 Introduction

In the analysis of switching surges on polyphase transmission systems, sequential pole closure problem should be taken into account. In practice, simultaneous pole closure of circuit breakers cannot be achieved.

A digital computer solution of the sequential transient problem involves a change in the system matrix with time. Therefore, the problem to be analysed becomes nonlinear. In the thesis, Fourier transform modal analysis method is extended to the solution of nonlinear problems arising from sequential pole closure when the system is

energized from an infinite busbar.

3.4.2 Application of Piecewise Fourier Transform Method

In evaluating the transient response of the multiconductor transmission system, the response of the system $f(t)$ in the time domain is obtained at discrete time intervals t_o. In the sequential pole closure problem the Fourier transform $F(w)$ corresponding to $f(t)$ is essentially found.

If time function $f(t)$ is divided into N strips, so that the strip width is small enough, the variation is approximated by a straight line. By using this form of approximation, it is possible to build up the Fourier transform of $f(t)$ by summing the transform of such strips.

Wedepohl and Mohamed [12] expressed the Fourier transform of the induced voltages as described in Appendix D.

The modified Fourier transform of the voltages imposed on the system as a result of first pole closure is easily obtained. Therefore, in the case of three phase sequential pole closure, the calculation of the system response is performed for the first pole closure, as if it is a single phase energisation. After a short time period from the first pole closure, the second pole closes and the third one follows. During the interval between the first pole and the second pole closure, a certain amount of energy transfer takes place between energized conductor and the other two conductors. When the second pole of the circuit breaker closes, the corresponding phase conductor acquires the instantaneous value of the supply voltage and remains unchanged for the

34

rest of the observation time. Meanwhile, the third conductor is still open, and acquires a new induced voltage until the third pole comes into operation. As soon as the third pole closes, the voltage on the third phase, then, corresponds to the supply voltage.

If we take T_1 as the closure time of the second pole, and T_2 as the closure time of the third pole and when the system is energized from an infinite busbar the steps of the transient solution can be described as follows.

Closure time of the first pole is taken as zero; system response is computed exactly the same as single phase energisation problem till time T_1. Second pole closes at time T_1. The new boundary conditions at the sending end are known on the first two conductors, and the third one is open circuit. System input matrix will be changed accordingly and the response is computed. For the solution to be valid from time zero, the modified Fourier transform of the voltage on the second conductor during the time interval $0 < t < T_1$ should be computed. Then the voltage on the second conductor is expressed in frequency domain using Piecewise Fourier Transform as mentioned in Appendix D and added to the modified Fourier transform of the supply voltage of the same conductor for the time interval $t < T_1$.

Time response of the cable conductors is computed over the time interval $T_1 < t < T_2$ taking into account the effects of energized conductors 1 and 2. Induced voltage on the third conductor is computed. Piecewise Fourier transform is derived numerically and added to the modified Fourier transform of the supply voltage for the same conductor for time $t < T_2$.

The flowchart of the computer program related to sequential pole closure when the system is energized from an infinite busbar is shown in Fig.3.1.
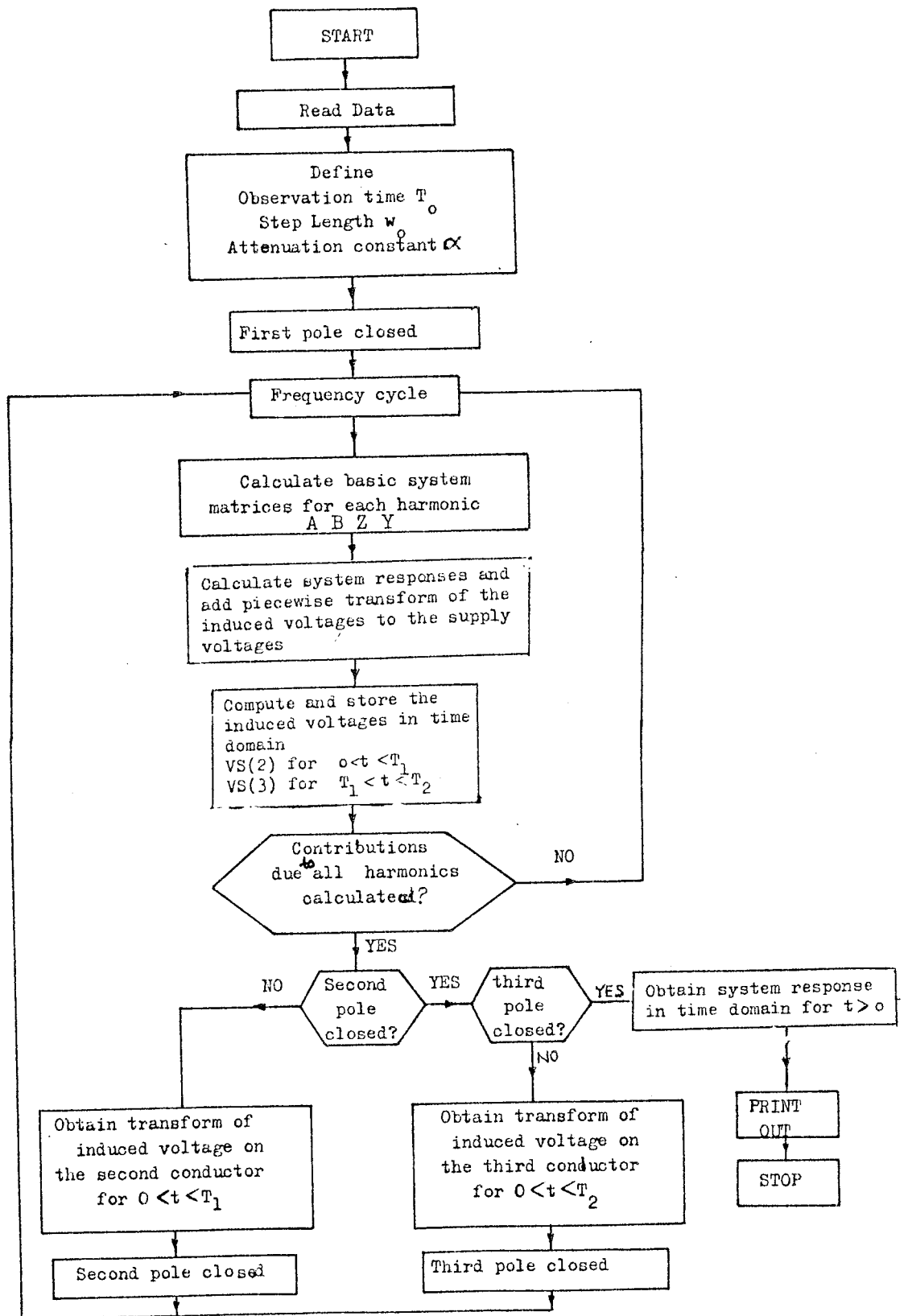
Fig.3.1 Flowchart for sequential pole closure problem

CHAPTER 4

SYSTEM STUDIES

The basic system studied is the crossbonded cable of
275 kV and sheaths are solidly interconnected and bonded
to earth at major section-ends. Configuration of the
single-core power cables is shown in Fig.4.1. The data
related to the individual phase cables is given in Table
4.1.

Total length of the cable is 27432 meters and the
number of major sections is 20. Earth is assumed to be
homogeneous with a resistivity of 20 ohm-meters. The
receiving end of the cable is open-circuited.

The modal parameters of the crossbonded cable is
shown in Table 4.2. The order in which the elements of the
characteristic impedance matrix arise, and also the order
in which the voltage and current eigenvectors arise, refer
to middle, right-hand and left hand side conductors, res-
pectively.

In the following sections, computer results of the
transient voltages along the cable system due to simultaneous
and sequential switch closures are presented. Effects of
cable length, source impedance, shunt compensation and
sequential pole closure on the magnitude of transient vol-
tages are studied. Maximum frequency harmonic, NF_{max} and
maximum time step, NT_{max} are given in each figure in the
system studies below.
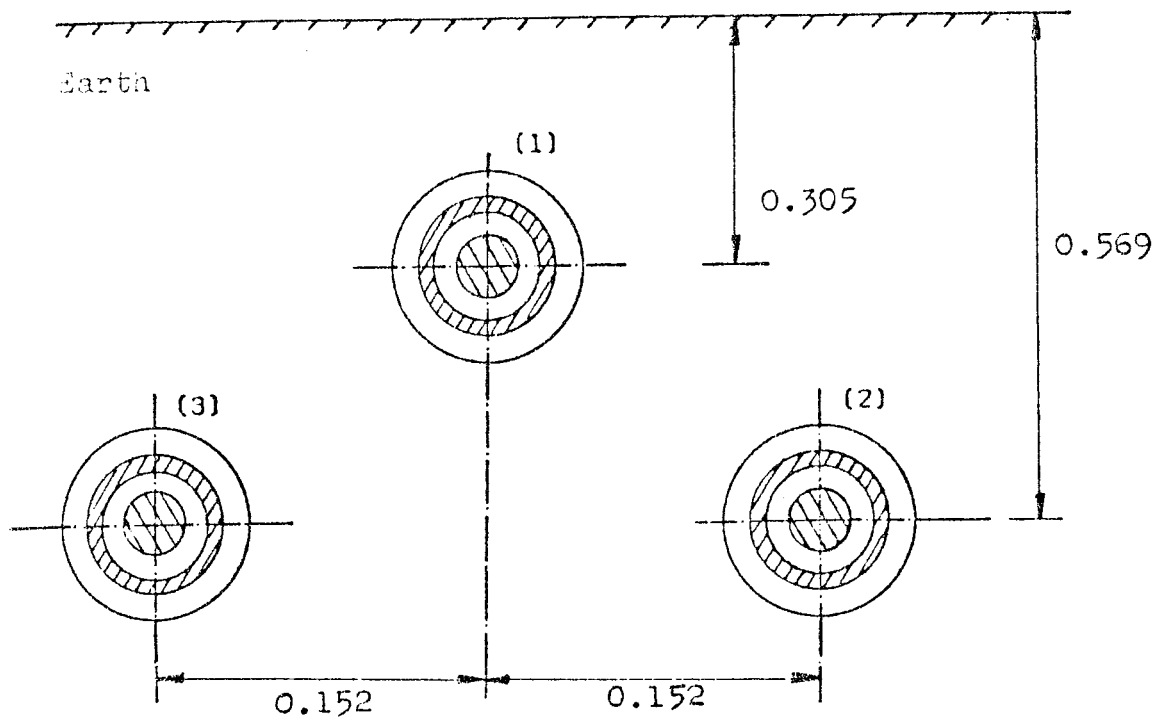
Fig.4.1 Configuration of the 275 kV cable system
(distances are in metres).

TABLE 4.1 CABLE DATA

Conductor radius   = 1.969 cm

Sheath inner radius   = 3.556 cm

Sheath outer radius   = 3.703 cm

Cable outer radius   = 4.115 cm

Resistivity of core   = 1.72×10^{-8} Ohm-m.

Resistivity of sheath   = 3.58×10^{-8} Ohm-m.

Relative permittivity
 of core insulation   = 3.72

Relative permittivity
 of sheath insulation   = 2.33

Relative permeability
 of the core and sheath   = 1.0

TABLE 4.2 MODAL PARAMETERS OF THE 275 KV CROSS-BONDED CABLE

Frequency = 50 Hz.   Earth resistivity = 20 Ohm-m.

Major Section Charactiristic Impedance Matrix Z_o (Ohm/$\underline{deg}$)

38.11 /$\underline{-11.44}$	6.70 / $\underline{-125.01}$	6.70 / $\underline{-125.01}$
6.70/$\underline{-125.01}$	38.11 / $\underline{-11.44}$	6.70 / $\underline{-125.01}$
6.70/$\underline{-125.01}$	6.70 / $\underline{-125.01}$	38.11 / $\underline{-11.44}$

Major Section Characteristic Admittance Matrix Y_o

(Milli Mho / $\underline{deg}$)

24.92 / $\underline{13.60}$	4.64 / $\underline{89.86}$	4.64 / $\underline{89.86}$
4.64 / $\underline{89.86}$	24.92 / $\underline{13.60}$	4.64 / $\underline{89.86}$
4.64 / $\underline{89.86}$	4.64 / $\underline{89.86}$	24.92 / $\underline{13.60}$

Mode No.	Eigenvectors Voltage	Current	Velocity km/sec	Attenuation db/km
	1.000 / $\underline{0.00}$	0.500 / $\underline{0.00}$		
1	0.000 / $\underline{0.00}$	0.000 / $\underline{0.00}$	69415	0.00197
	1.000 / $\underline{180.00}$	0.500 / $\underline{180.00}$		
	0.500 / $\underline{180.00}$	0.333 / $\underline{180.00}$		
2	1.000 / $\underline{0.00}$	0.667 / $\underline{0.00}$	69415	0.00197
	0.590 / $\underline{180.00}$	0.333 / $\underline{180.00}$		
	1.000 / $\underline{0.00}$	0.333 / $\underline{0.00}$		
3	1.000 / $\underline{0.00}$	0.333 / $\underline{0.00}$	96407	0.01768
	1.000 / $\underline{0.00}$	0.333 / $\underline{0.00}$		

4.1 Single Phase Energisation

In case of single phase unit step energisation, transient response is obtained for the observation time of 1 mili-second and harmonic responses are evaluated for 250 frequency harmonic values.

The cable is energized from the first conductor with a l.p.u. step voltage. There is no compensation and no trapped charges on the cable.

Wave propagation along the cable may be explained taking into account the receiving-end conditions. Since the receiving-end of the cable is open-circuited, the voltage waves, upon arrival, are doubled and a voltage of 2.142 p.u. is produced at the receiving-end . Fig.4.2 (a) and (b) show the waveform of the sending-end and receiving-end voltages, respectively, when the system is energized from an infinite bus-bar.

At the sending-end, the induced voltages on the unenergized conductors acquire negative values first. The ratio of magnitudes of induced voltages to unit step voltage is found as -0.180 p.u. from Fig.4.2 (a) before the reflected waves arrive at the sending-end. This complies with the ratio of the cable mutual-to-self surge impedances(i.e.)—.176 at 50 Hz as can be calculated from Table 4.2.

At the receiving-end, the induced voltages on the unenergized conductors acquire positive values first, and then acquire negative values as shown in Fig.4.2 (b)

Sending-end voltages, obtained initially, as can be seen in Fig.4.2(a) may be written in vector form as

$$
\underset{\sim}{V}_S = \begin{bmatrix} 1.000 \\ -0.200 \\ -0.200 \end{bmatrix}
$$

The modal voltage vector $\underset{\sim}{V}^{(m)}$ is determined as

$$
\underset{\sim}{V}^{(m)} = Q^{-1} \; \underset{\sim}{V}_S = \begin{bmatrix} \frac{1}{2} & 0 & -\frac{1}{2} \\ -\frac{1}{3} & \frac{2}{3} & -\frac{1}{3} \\ \frac{1}{3} & \frac{1}{3} & \frac{1}{3} \end{bmatrix} \begin{bmatrix} 1.000 \\ -0.200 \\ -0.200 \end{bmatrix} = \begin{bmatrix} 0.60 \\ -0.40 \\ 0.20 \end{bmatrix}
$$

where Q^{-1} is the inverse eigenvector matrix as given in Appendix C. Thus, the sending-end voltages may be shown to be made up of the following components,

$$
\underset{\sim}{V}_S = Q \; \underset{\sim}{V}^{(m)} = \underbrace{0.60 \begin{bmatrix} 1 \\ 0 \\ -1 \end{bmatrix}}_{\text{mode 1}} \underbrace{-0.40 \begin{bmatrix} -\frac{1}{2} \\ 1 \\ -\frac{1}{2} \end{bmatrix}}_{\text{mode 2}} \underbrace{+ 0.20 \begin{bmatrix} 1 \\ 1 \\ 1 \end{bmatrix}}_{\text{mode 3}}
$$

where Q is the eigenvector matrix (modal transformation matrix) as given in Appendix C. Modes 1 and 2 are differential modes between the cable cores, and mode 3 is the core-to-sheath coaxial mode. Mode 3 has the highest velocity as can be seen from Table 4.2. Therefore it arrives at the receiving-end first. Velocities of modes 1 and 2 are the same and they arrive at the receiving-end in 395 micro-second. This calculated travel time complies with that of the unit step response of the cable shown in Fig.4.2.(b) in which, upon the arrival of differential modes

42

to the receiving-end, the voltage at this end rises abruptly to 1.760 p.u.

If a sinusoidal voltage is applied to first phase, the voltage waveforms obtained at the sending-end and receiving-end within 20 ms, taking the number of the frequency harmonics as 150 , are as shown in Fig.4.3 (c) and (d). Maximum overvoltage at the receiving-end of the first conductor is 2.073 p.u. When the calculations are carried out for the maximum frequency harmonics of 50 with 100 maximum time steps,for the observation time of 20 ms, the voltage waveforms obtained at the sending-end and receiving-end are as shown in Figs.4.3(a) and (b) respectively.

4.2 Three-phase Energisation

4.2.1 Effect of Cable Length

Effect of cable length on the magnitude of switching transient overvoltages has been studied in the case of three-phase simultaneous energisation from an infinite bus-bar. In the system, the length of each major section is taken to be 1371.6 meters. Studies have been carried out on different cables which consist of 15,20,25 and 30 major sections.

Receiving-end voltage waveforms obtained for different cable lengths are shown in Fig.4.4(a),(b),(c), (d). Variation of the maximum receiving-end voltage with the cable length is tabulated in Table 4.3. As can be seen from the table, the magnitude of the maximum receiving-end voltage for the first phase decreases with the increase in cable length while the the magnitudes of the second and third phase receiving-end voltages increase with the increase in cable length.

43

TABLE 4.3 RELATION BETWEEN MAXIMUM OVERVOLTAGE AND THE CABLE LENGTH

Number of major sections	Cable length l(m)	Maximum magnitude of the receiving -end voltages (p.u.)		
		phase 1	phase 2	phase 3
15	20574	1.982	1.442	1.352
20	27432	1.980	1.474	1.377
25	34290	1.973	1.525	1.376
30	41148	1.961	1.547	1.428

4.2.2 Switching Surges Along the Crossbonded Cable

Figs.4.5 (a),(b) and (c) show variation of switching overvoltages at the 10th and 15th major sections and at the receiving-end of the cable. The variation of the overvoltage magnitude along the cable can be explained by travelling wave phenomena. At the receiving-end, voltage waves are reflected by the reflection coefficient of (+1) and doubled. Modes with different velocities cancel each other at some intermediate points of the cable since two of them may travel towards the receiving-end while the other one(mode 3) is travelling towards the sending-end. The amount of cancellation is not constant since mode 3 is highly dependent upon the frequency.

As can be seen from the results, the magnitude of overvoltages increases gradually as the intermediate point of interest moves away from the sending-end.

44

4.2.3 Effect of Source Impedance

As source inductane increases, the frequency of oscillations decreases. Therefore the system tends to go into resonance as the dominant frequency of the system voltage approaches the supply frequency. This causes higher voltages at both sending-end and receiving-end of the cable as can be seen from Figs.4.6, 4.7,4.8,4.9. Variation of the maximum overvoltage at the sending and receiving ends within 20 ms with the source inductance is tabulated in Table 4.4. As can be seen from Figs.4.8 and 4.9 that,system tends to go into resonance when source inductance is 0.24 H and 0.48 H, respectively.

TABLE 4.4 VARIATION OF MAXIMUM MAGNITUDES OF OVERVOLTAGES WITH THE SOURCE INDUCTANCE

Source Inductance (Henry)	Maximum Sending-end Voltage (p.u.)			Maximum Receiving-end Voltage (p.u.)		
	phase 1	phase 2	phase 3	phase 1	phase 2	phase 3
0.016	1.566	1.280	1.275	1.904	1.455	1.447
0.048	1.864	1.492	1.435	2.017	1.577	1.518
0.24	2.535	1.812	1.940	2.587	1.845	1.974
0.48	3.582	2.986	3.049	3.625	3.021	3.084

If energisation is done from an infinite bus-bar, inductance is zero and the sending-end voltages are the same as the source voltages. When the source inductance is introduced to the system, sending-end voltages exceed the source voltage due to the reflection of travelling waves at the source inductance.

For the inductive source, the voltage waves rise exponentially with a time constant which is directly proportional to the source inductance. The corrosponding frequency of oscillations which are superimposed on the power frequency component decreases with the increasing inductance values. For example, the frequency of oscillations for 0.016 henry source is approximately 330 Hz; however it is 220 Hz for 0.048 henry source, 150 Hz for 0.24 henry source and 60 Hz for 0.48 henry source as can be seen from Figs.4.6, 4.7. 4.8, and 4.9.

4.2.4 Effect of Shunt Compensation

Shunt reactor compensation is used in general to reduce the magnitudes of the switching surges.

Shunt compensation is employed here to minimize the overvoltages when the dominant frequency of the system approaches the supply frequency. Application of shunt compensation is found to be efficient. When the shunt reactors are used at sending-end and at both ends of the crossbonded cable, respectively, magnitude of overvoltages at both ends are observed to be reduced.

In system studies, the effect of shunt compensation on the magnitude of the transient overvoltages, is studied under three-phase simultaneous energisation from a source of 0.48 henry. Maximum overvoltage magnitude without shunt compensation is 3.625 p.u. within 20 ms, as can be seen from Fig.4.9. This overvoltage magnitude at the receiving-end decreases to values of 1.768 p.u. and 1.150 p.u. when 1.2 henry (200 MVar) shunt compensation is employed at the sending-end and at both ends of the cable, respectively. The related voltage waveforms can

be seen from Figs,4.10 and 4.11. When 2.4 henry (100 MVar) shunt compensation is considered at the sending-end, the maximum overvoltage magnitude comes out to be 1.171 p.u. at the receiving-end, as shown in Fig.4.12. If we use 2.4 henry shunt compensation at both ends of the cable, the magnitude of the maximum overvoltage becomes 0.653 p.u. at the receiving-end as shown in Fig.4.13. Further increase in the inductance of the shunt reactor decreases the magnitude of the maximum overvoltage in the system.

4.2.5 Effect of Sequential Pole Closure

In the studies of sequential energisation of the cable system from an infinite bus-bar, first phase breaker pole closes first, then the second and third one follow. Until the second pole closes, voltages are induced in the second and third conductor. Immediately, after the closure of the second pole, the voltage appearing on that conductor at the sending-end is the supply voltage. The effect of the second pole closure on the third conductor is taken into account. When the third pole closes, the voltage appearing on the corresponding conductor at the sending-end becomes the supply voltage.

In the studies, closure times of the second and third conductors have been chosen for two different conditions : (a) To close all the poles when corresponding phase voltages are at the peak values. Closure times are 3.2 and 6.6 ms for the second and third poles, respectively. (b) To close the second and third poles when the corresponding phase voltages pass through zero. Closure times are 8.4 and 11.6 ms for the second and third poles, respectively.
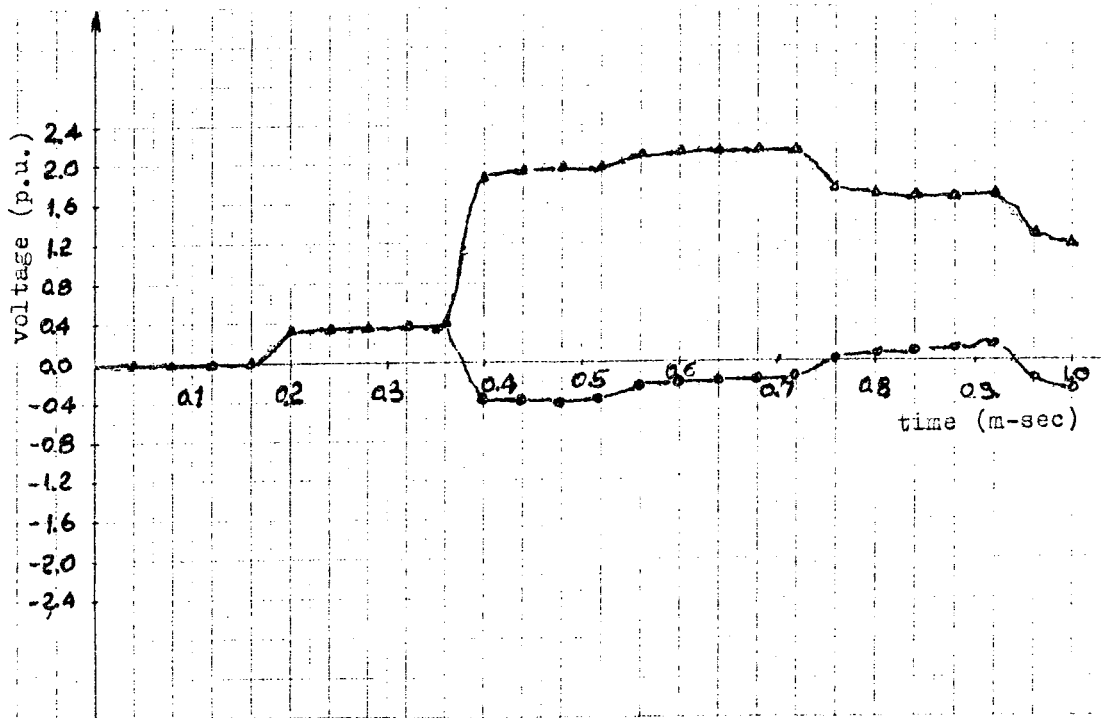
If the voltage responses are obtained for each of these conditions with the system fed from an infinite busbar, it is

found that in case of (b) smaller overvoltages arise at the sending-end and at the receiving-end as shown in Figs. 4.14(a),(b) and 4.15(a),(b). In case of pole closing instants 3.2 and 6.6 ms, the receiving-end maximum overvoltage reaches 2.38 p.u. within 20 ms with 150frequency harmonics. This magnitude is higher than the maximum receiving-end overvoltage (1.980 p.u.) obtained in simultaneous energisation within 20 ms with 150 maximum frequency harmonics as shown in Table 4.3.Fig.4.15(b) shows smaller overvoltages occur when the second and third poles close at the instant when the corresponding voltages are passing through zero.

In the single-phase energisation, the voltages at the sending-end and at the receiving-end are the same as those of the sequential energisation till the time of second pole closure as shown in Figs.4.3(c),(d) and 4.14(a),(b).
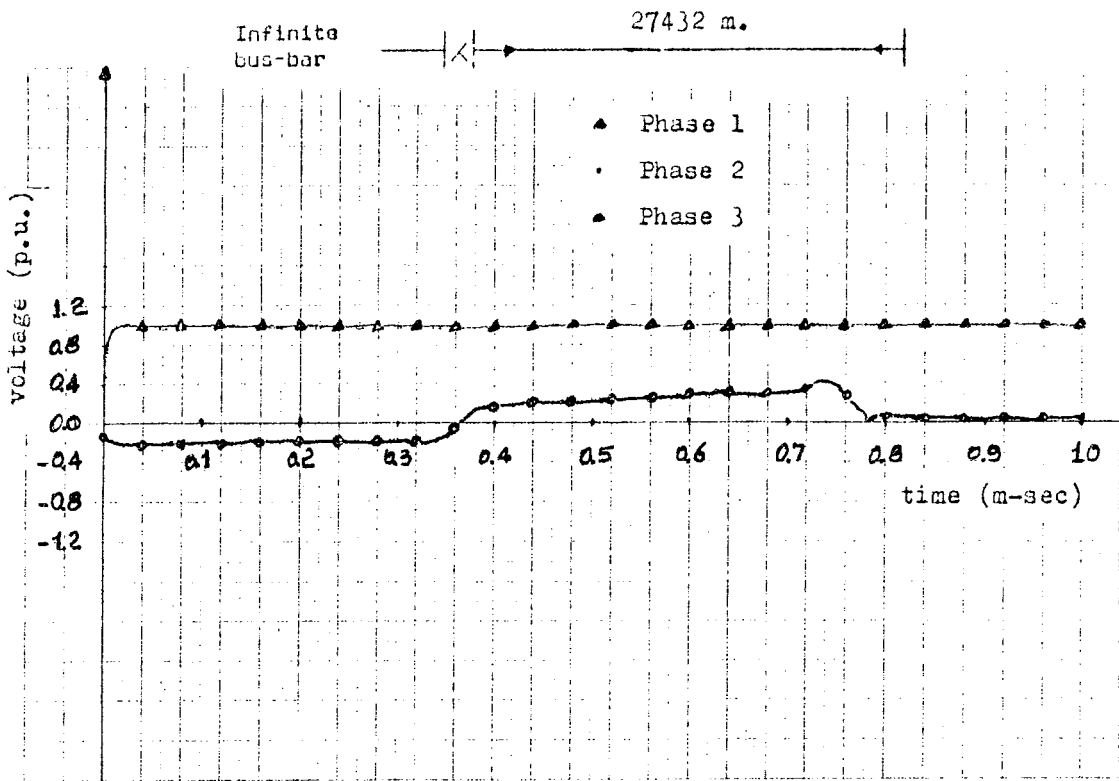
(a) Sending-end voltages

(b) Receiving-end voltages

Fig.4.2 Single phase unit step energisation, NF_{max} = 250,

NT_{max} = 500

49

Infinite bus-bar ⊢|×|⊣ 27432 m.

△ phase 1
. phase 2
⊕ phase 3

voltage (p.u.)

time (m-sec)

(a) Sending-end voltages

voltage (p.u.)

time (m-sec)
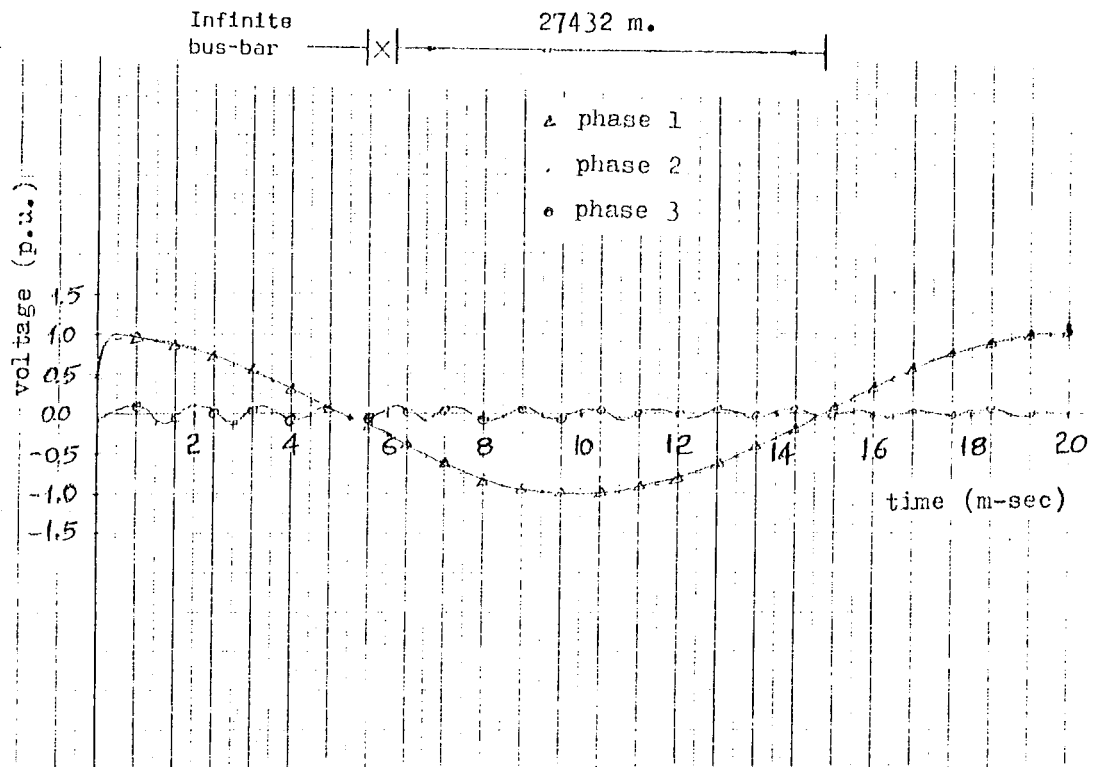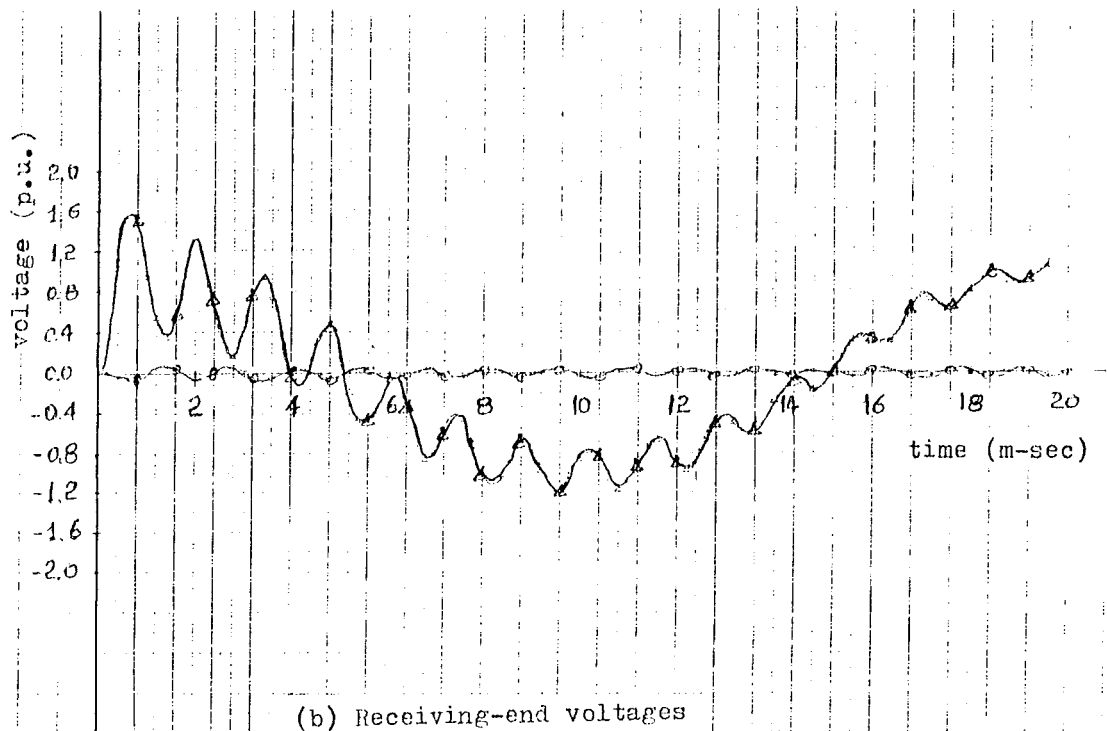
(b) Receiving-end voltages

Fig.4.3 Single phase sinusoidal energisation

, $NF_{max} = 50$, $NT_{max} = 100$
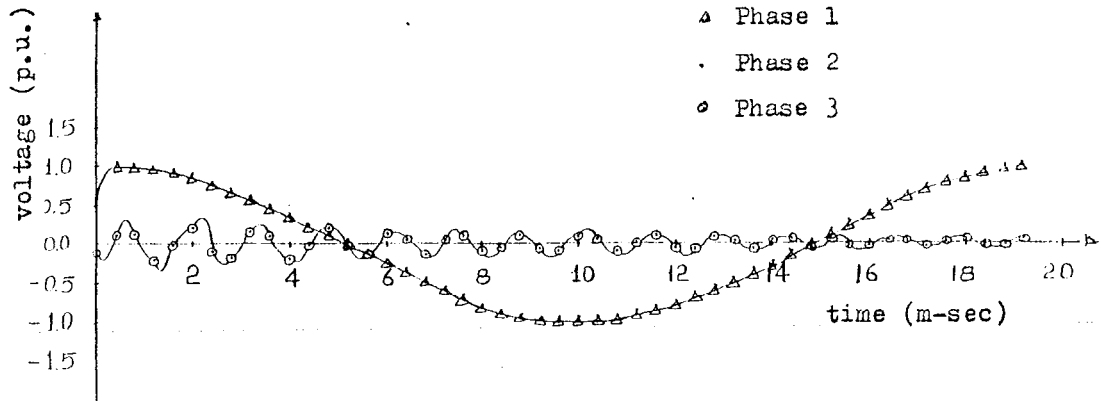
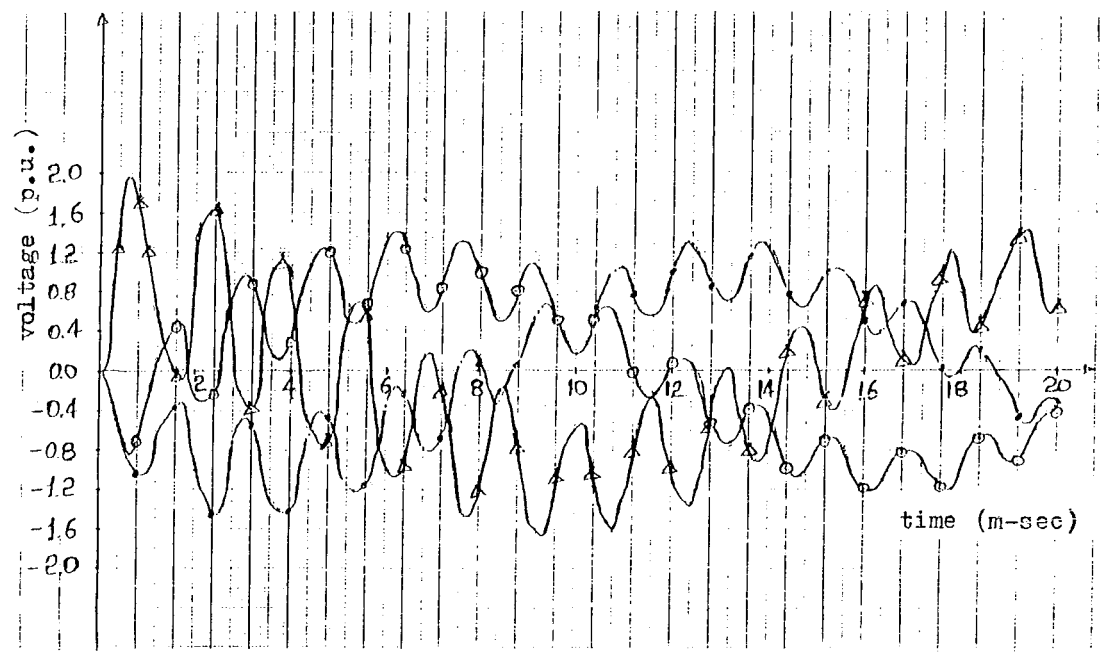(c) Sending-end voltages with $NF_{max} = 150$, $NT_{max} = 200$
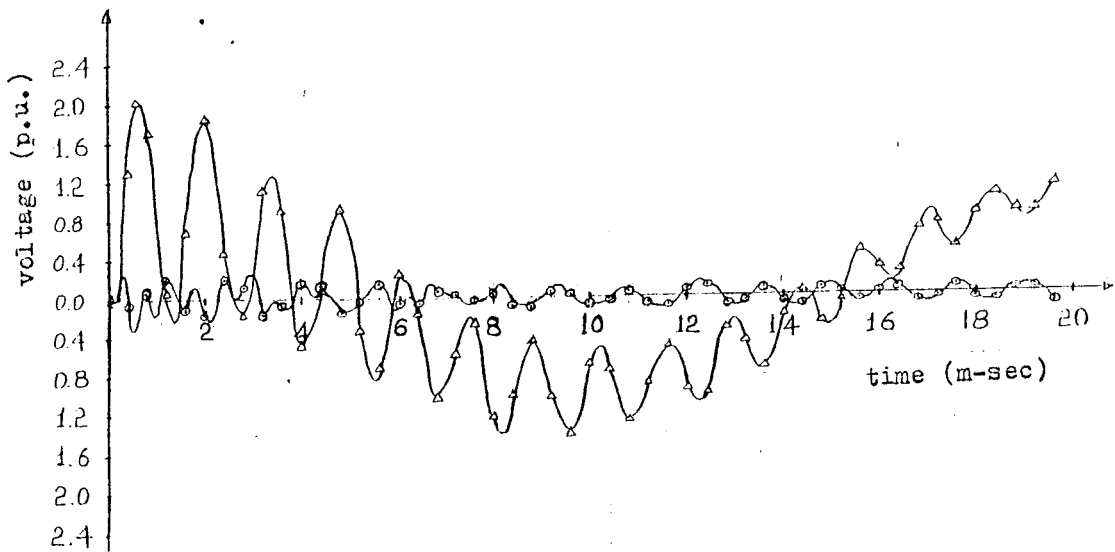
(d) Receiving-end voltages with $NF_{max} = 150$, $NT_{max} = 200$

Fig.4.3 (continued)
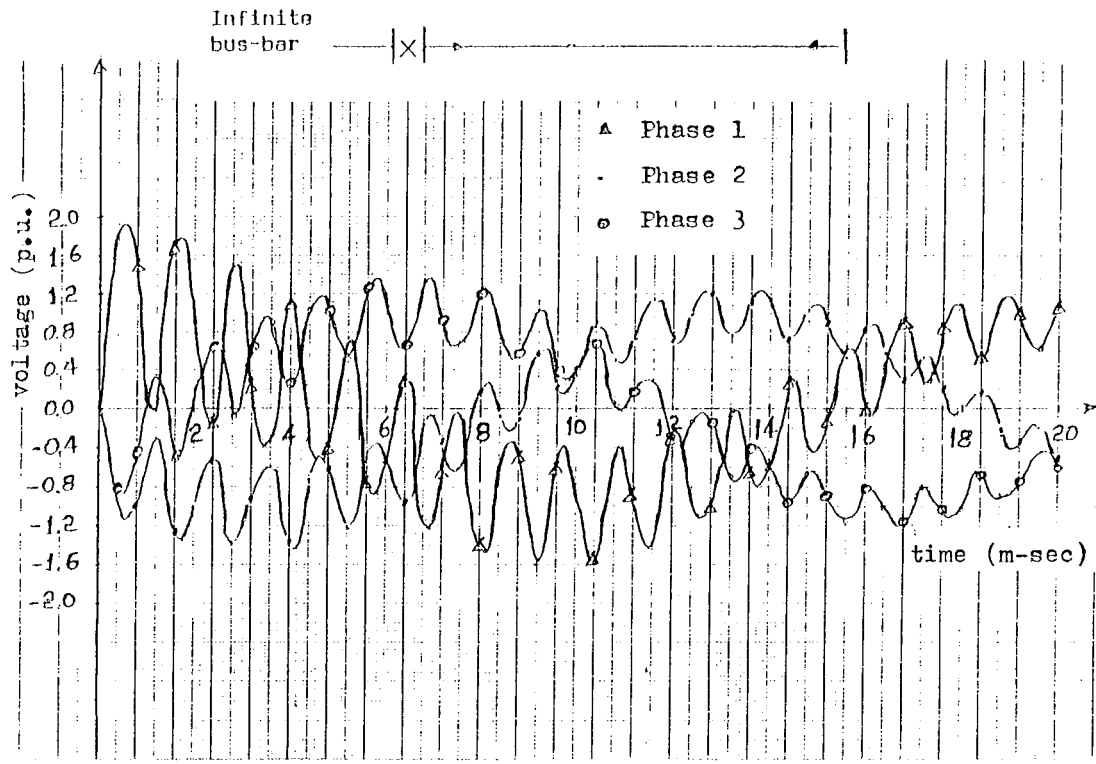
(a) Receiving-end voltages with the cable consisting
of 15 major sections (20574 m.)

(b) Receiving-end voltages with the cable consisting
of 20 major sections (27432 m.)

Fig.4.4 Effect of cable length on switching transients, NF_{max} =150,
NT_{max} = 200
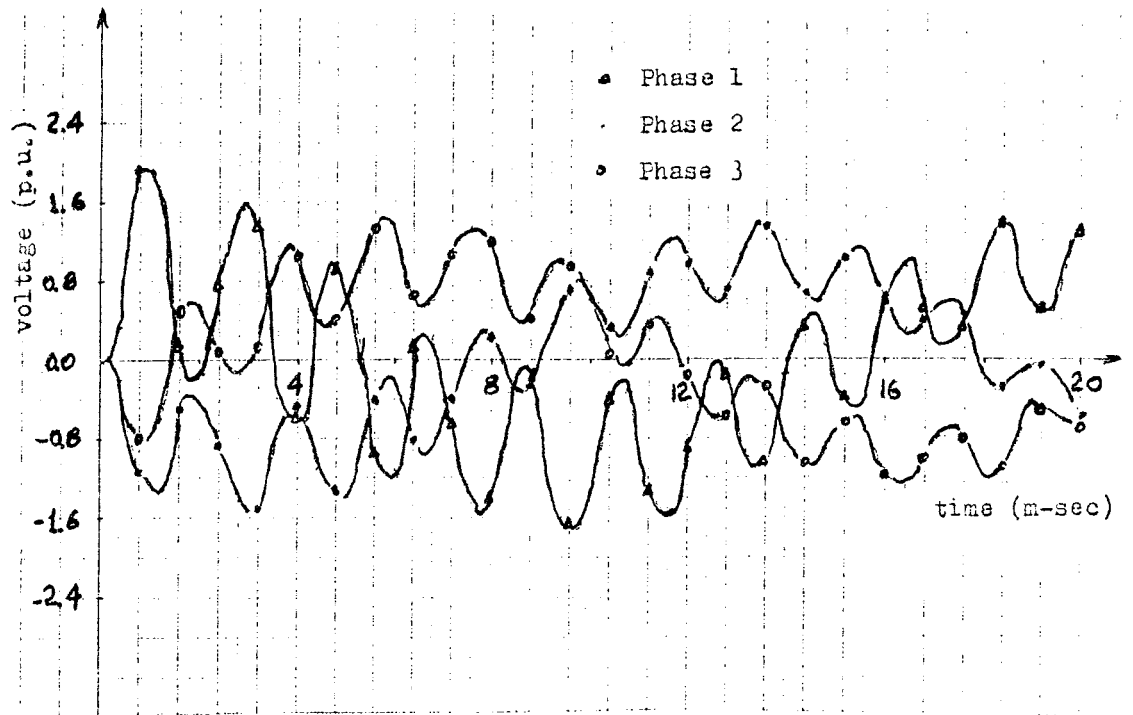
(c) Receiving-end voltages with the cable consisting
of 25 major sections (34290 m.)
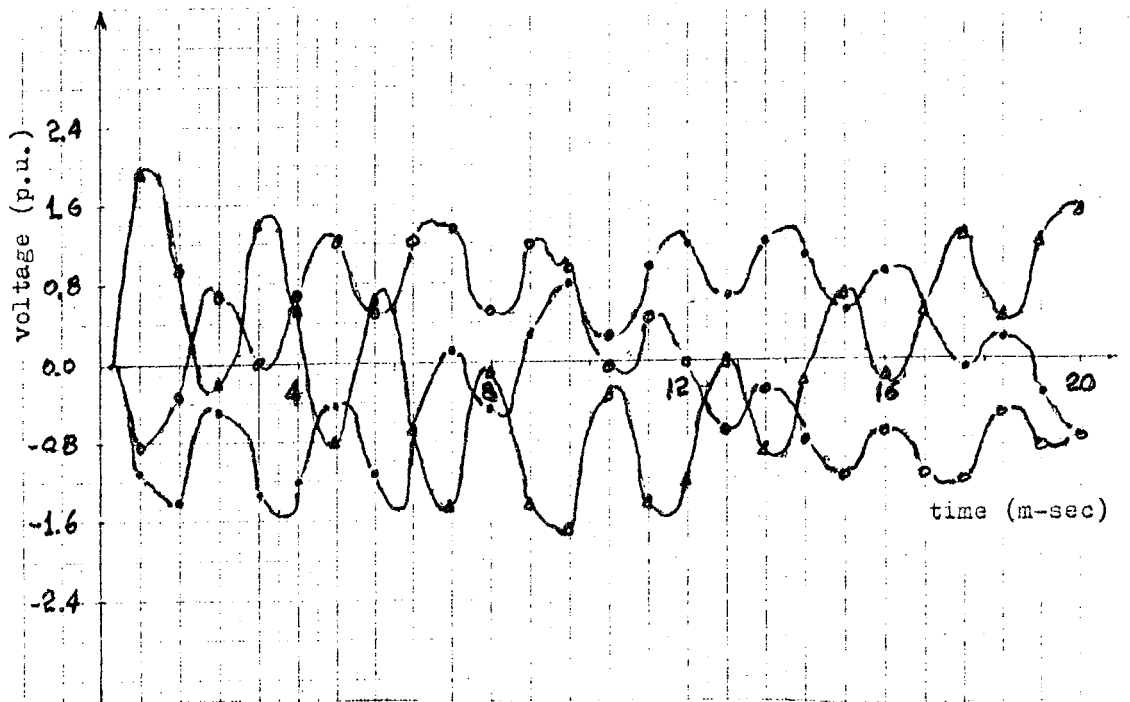
(d) Receiving-end voltages with the cable consisting
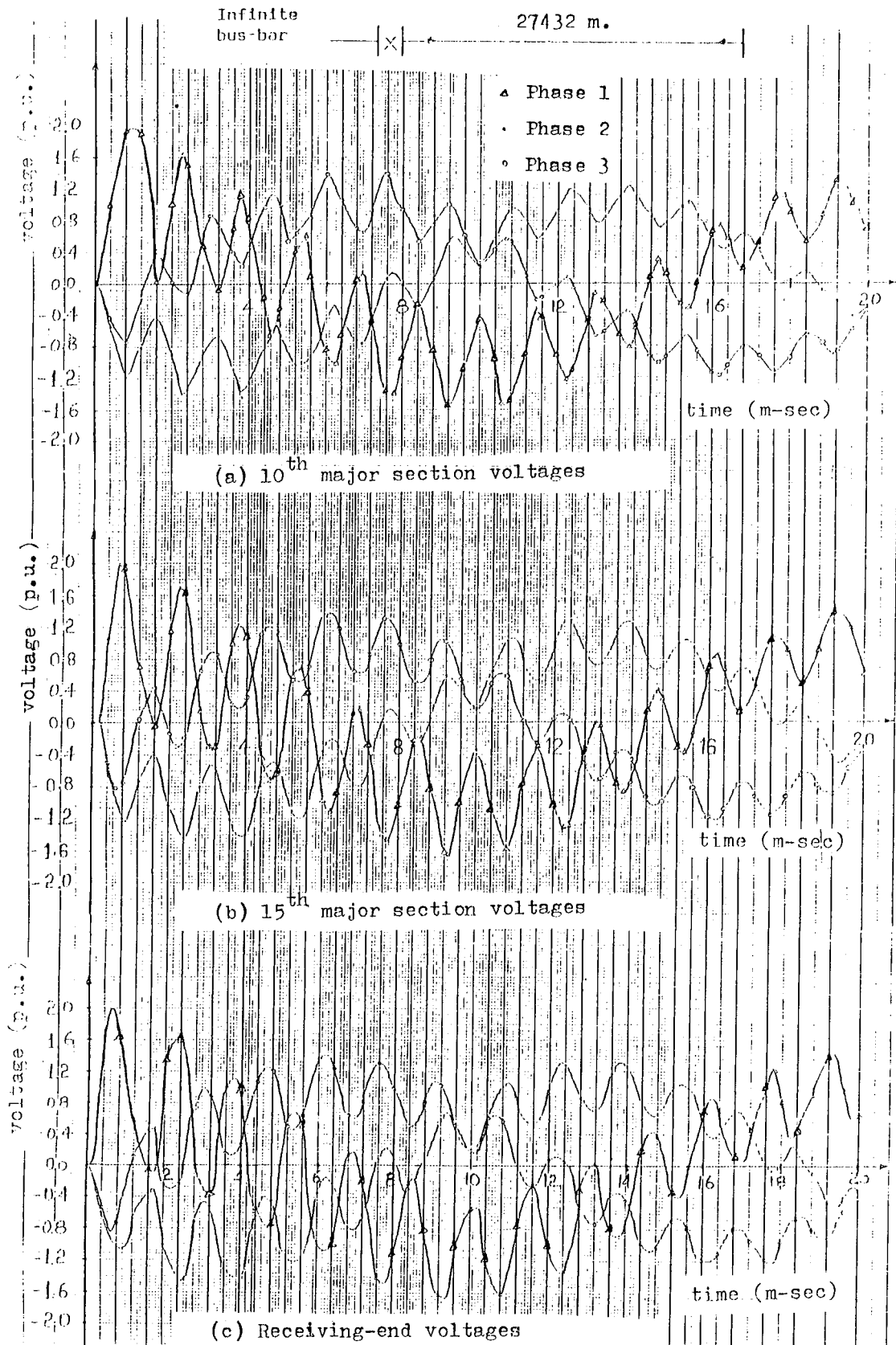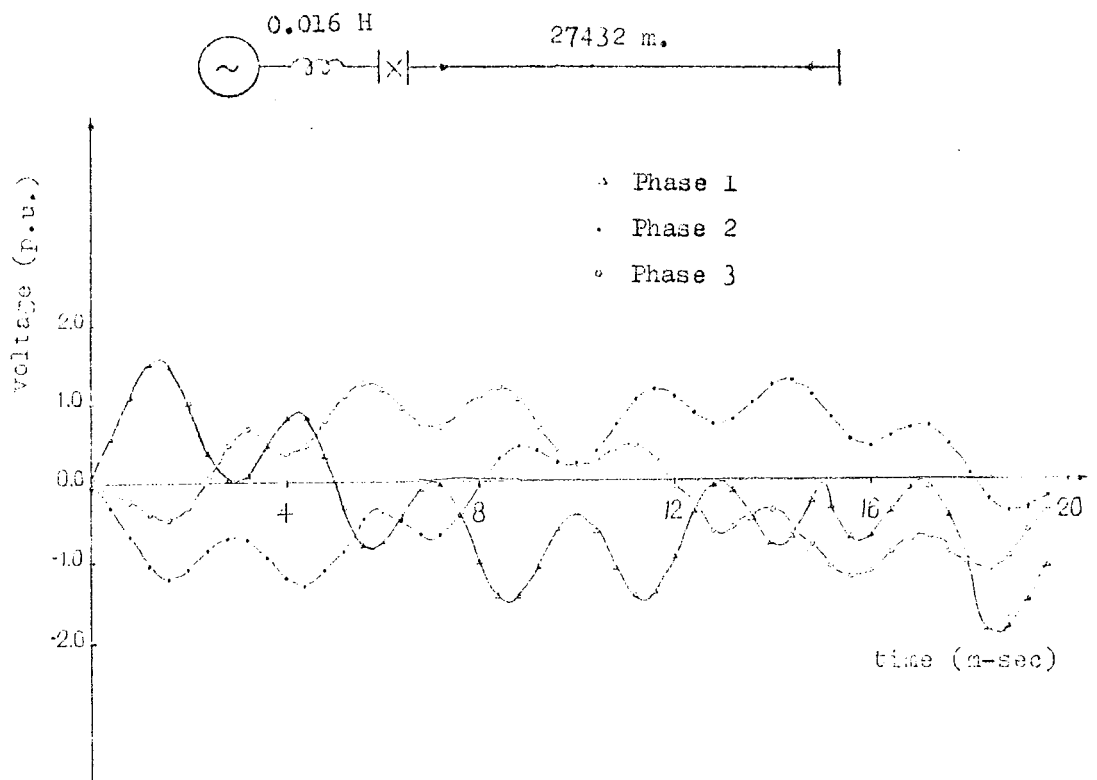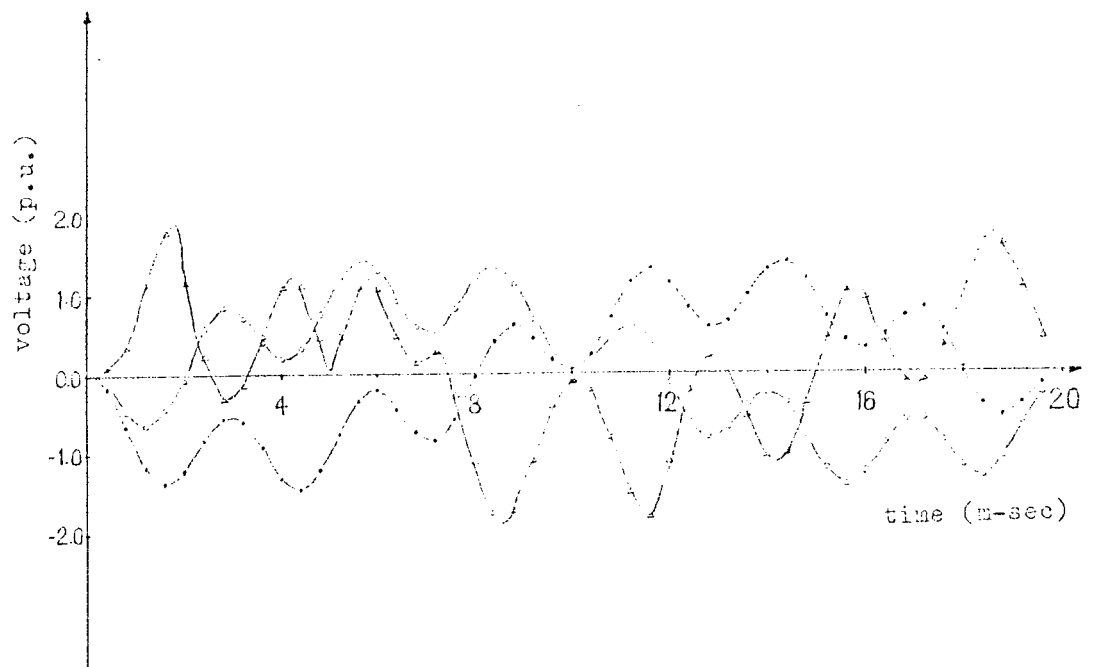of 30 major sections (41148 m.)

Fig.4.4 (continued)

53

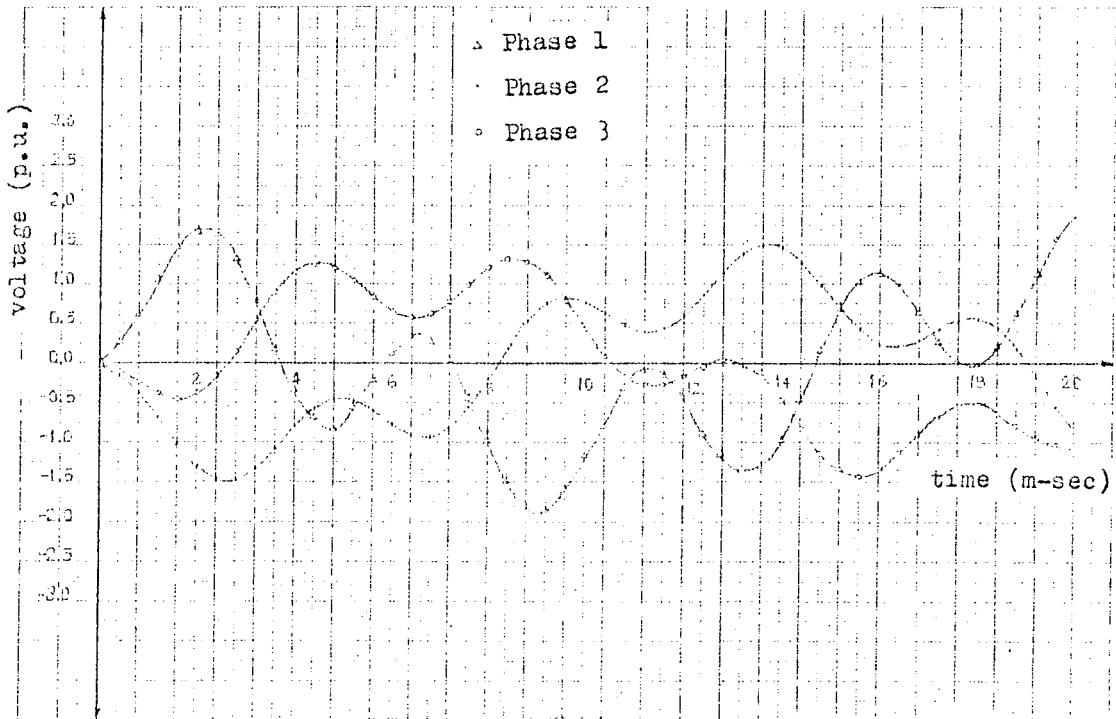Fig.4.5 Switching surges along the cable, $NF_{max} = 150$, $NT_{max} = 200$
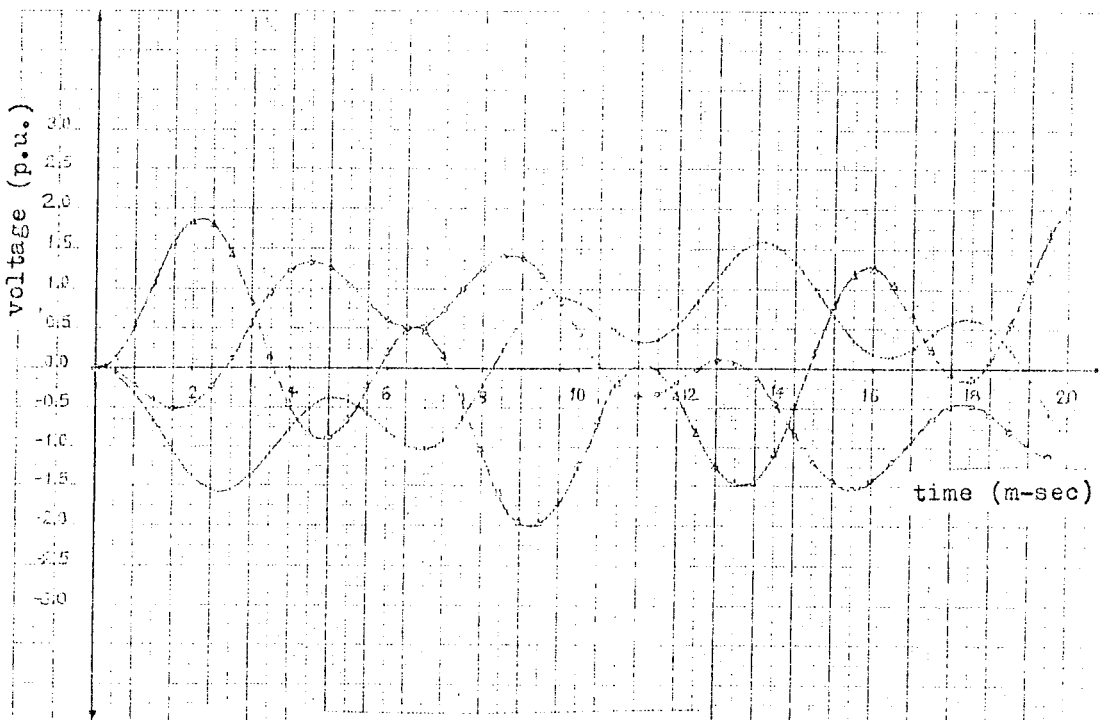
(a) Sending-end voltages

(b) Receiving-end voltages

Fig.4.6 Switching transients with 0.016 henry source inductance

$NF_{max} = 50$, $NT_{max} = 100$

(a) Sending-end voltages

(b) Receiving-end voltages

Fig.4.7 Switching transients with 0.048 henry source inductance
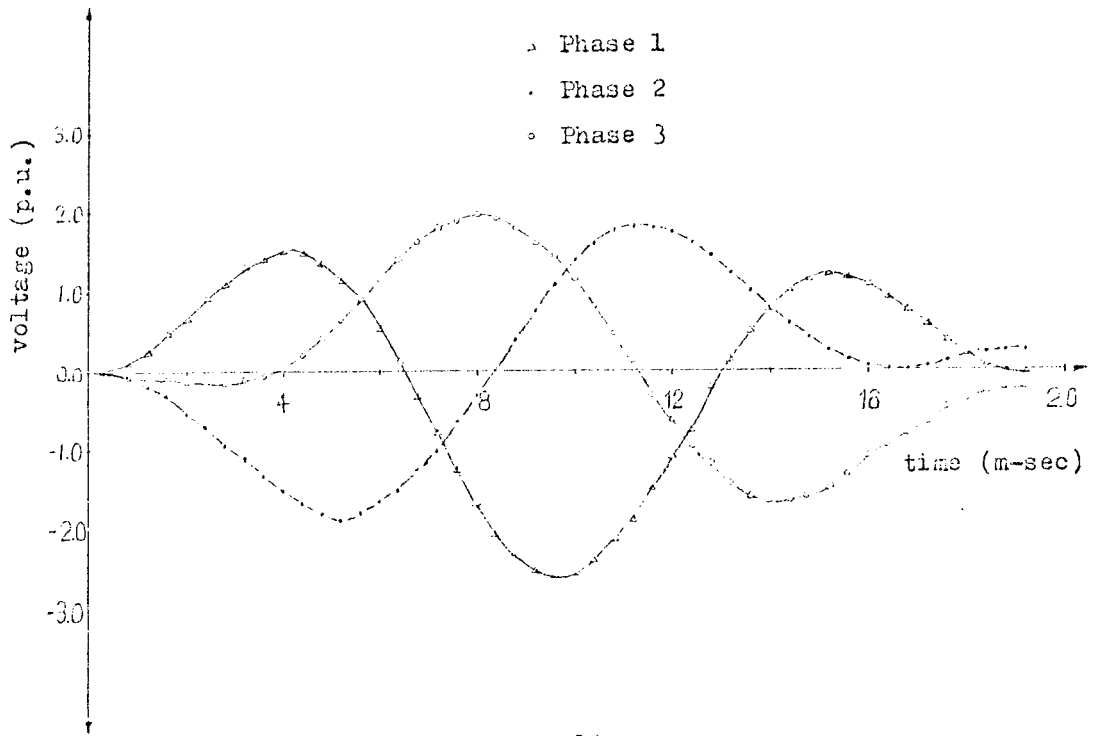
$NF_{max} = 50$, $NT_{max} = 100$
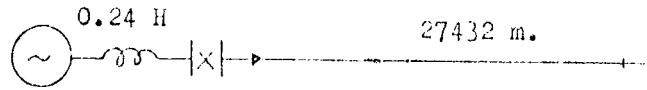
(a) Sending-end voltages
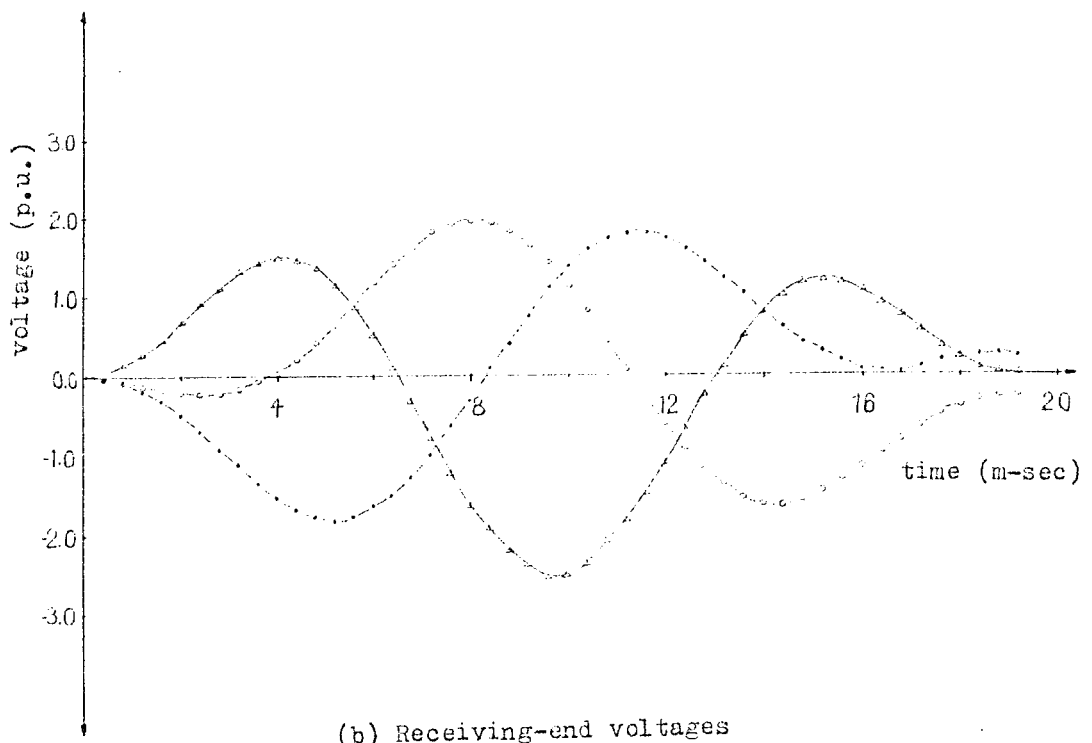
(b) Receiving-end voltages

Fig.4.8 Switching transients with 0.24 henry source inductance
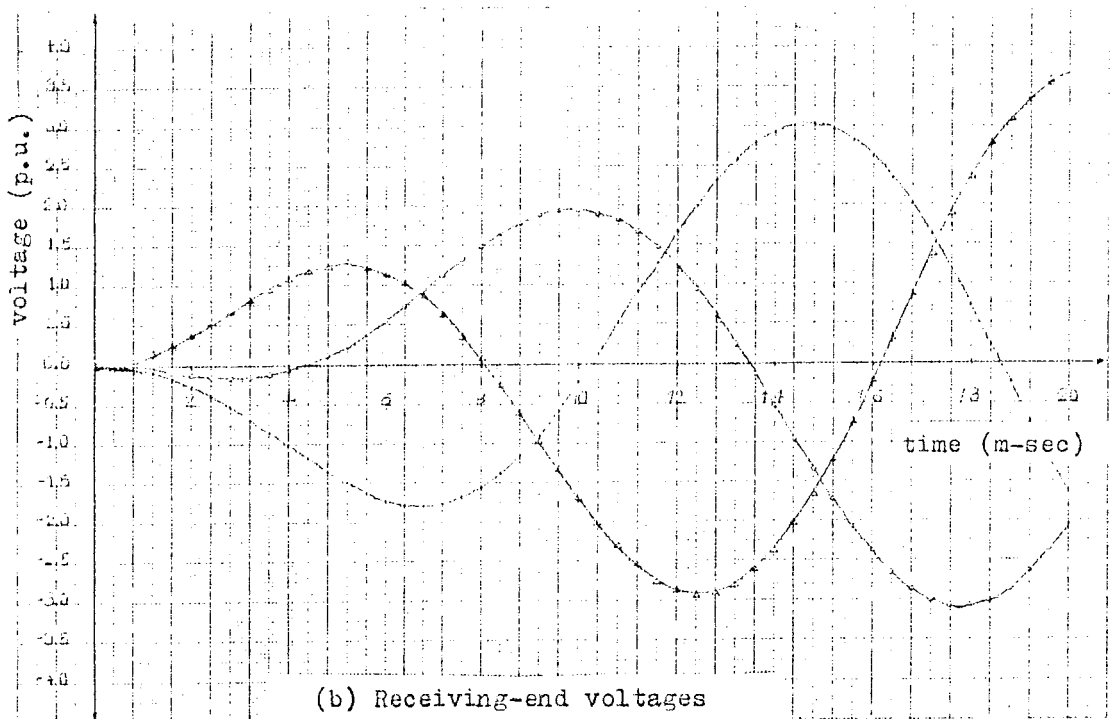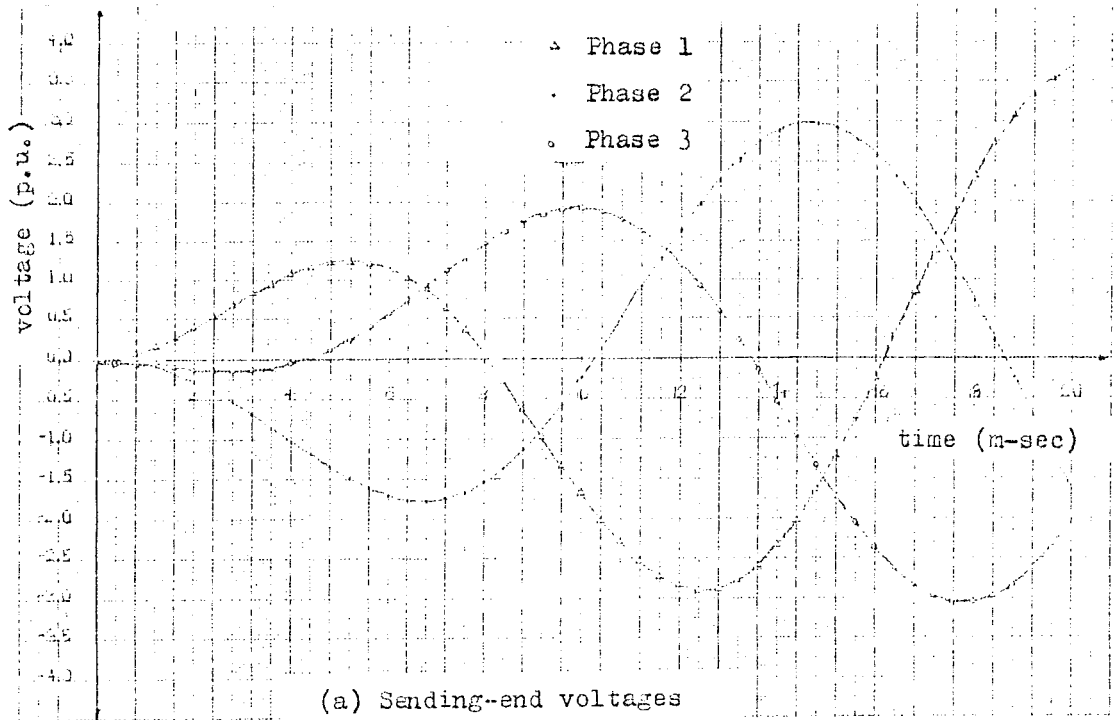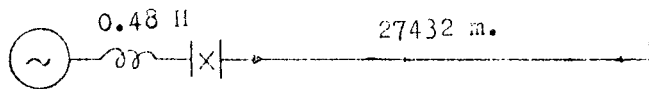
$NF_{max} = 50, \quad NT_{max} = 100$

Fig.4.9 Switching transients with 0.48 henry source inductance
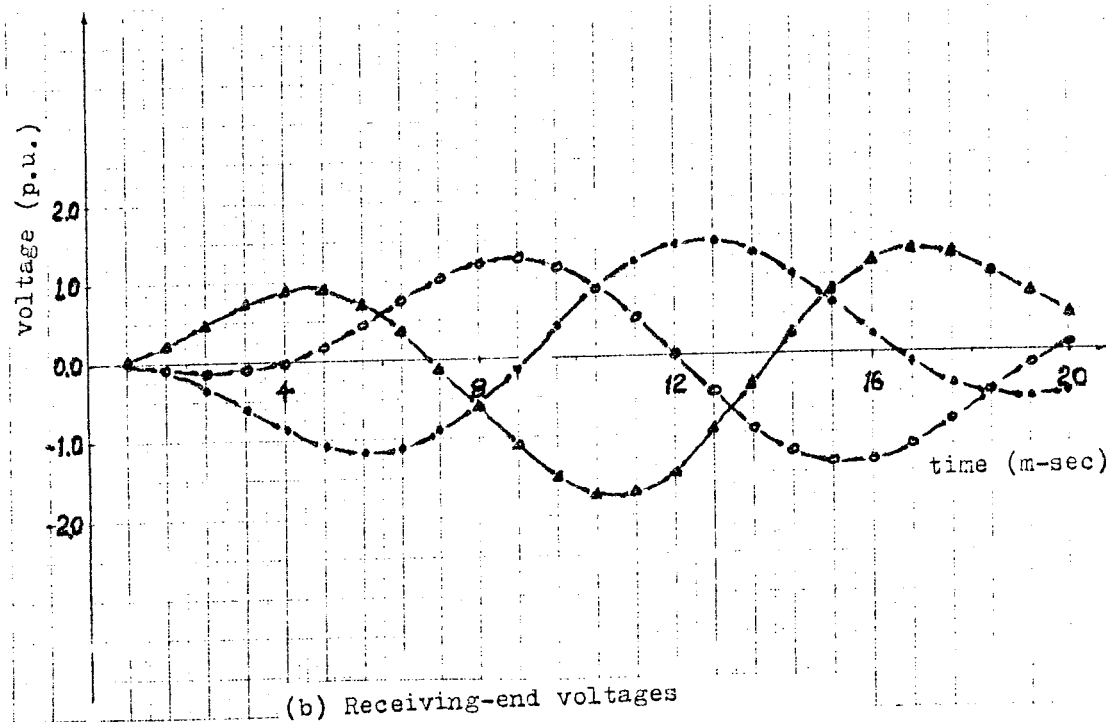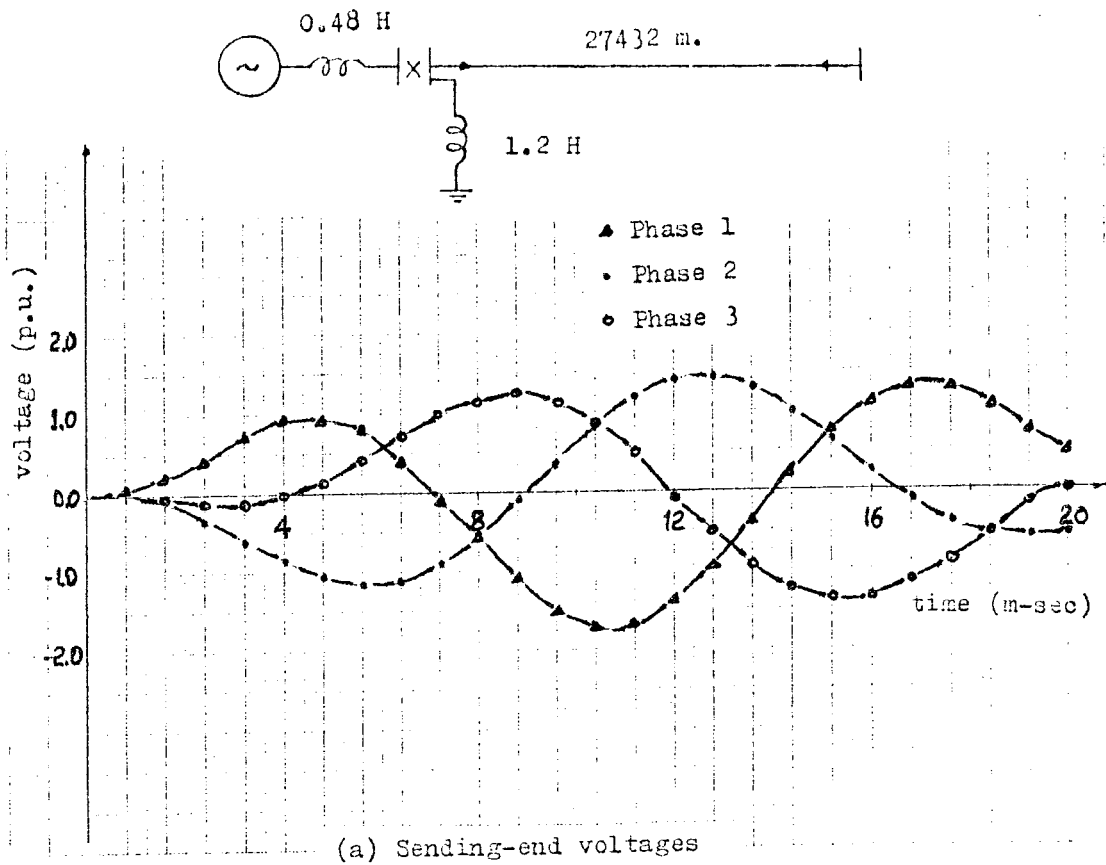
$$NF_{max} = 50, \quad NT_{max} = 100$$

Fig.4.10 Switching transients with 1.2 henry(200 MVar)shunt
compensation at the sending-end (source inductance = 0.48 H)
$NF_{max} = 50$, $NT_{max} = 100$

59
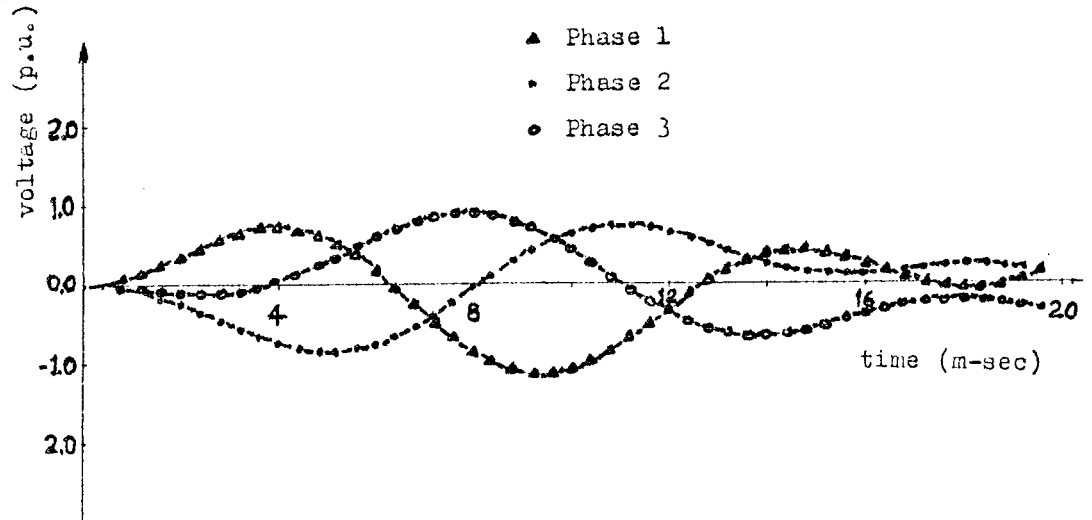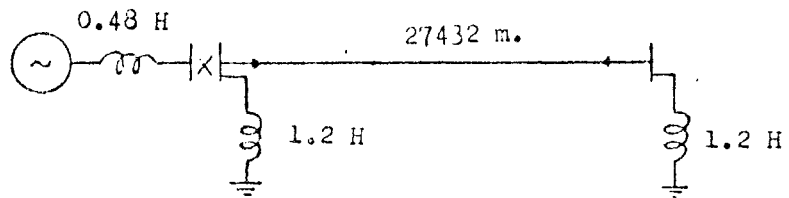
(a) Sending-end voltages
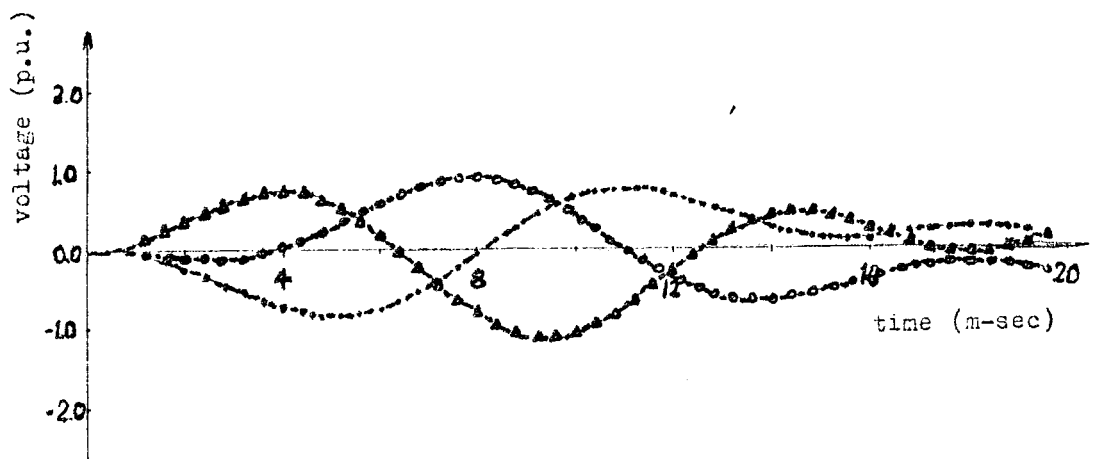
(b) Receiving-end voltages

Fig.4.11 Switching transients with 1.2 henry (200 MVar) shunt
compensation at both ends(source inductance = 0.48 H)

$NF_{max} = 50$, $NT_{max} = 100$
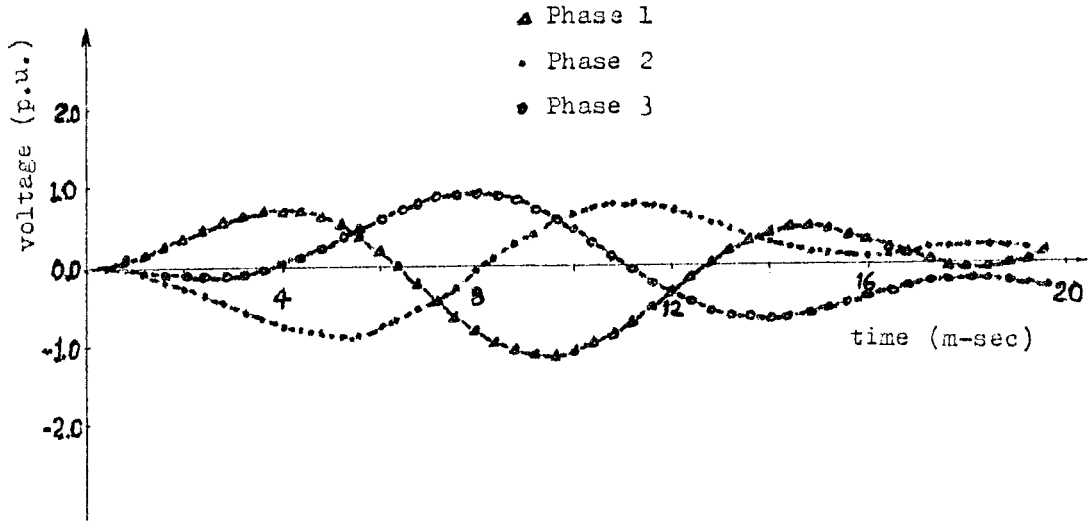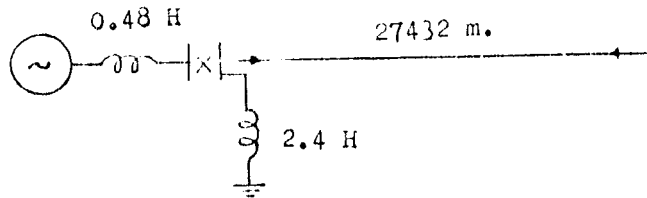
(a) Sending-end voltages
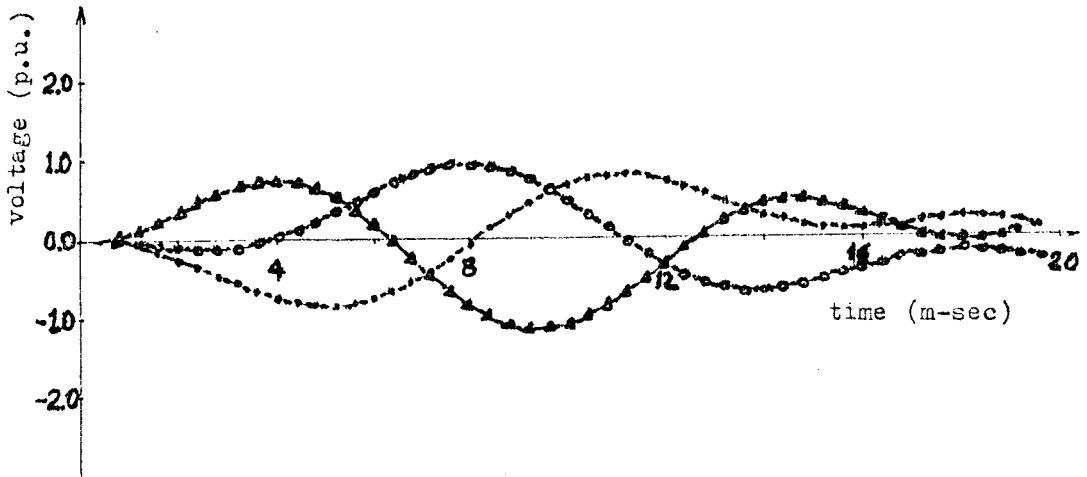
(b) Receiving-end voltages

Fig.4.12 Switching transient with 2.4 henry (100 MVar) shunt
compensation at the sending-end (source inductance = 0.48 H)

$NF_{max} = 50$, $NT_{max} = 100$
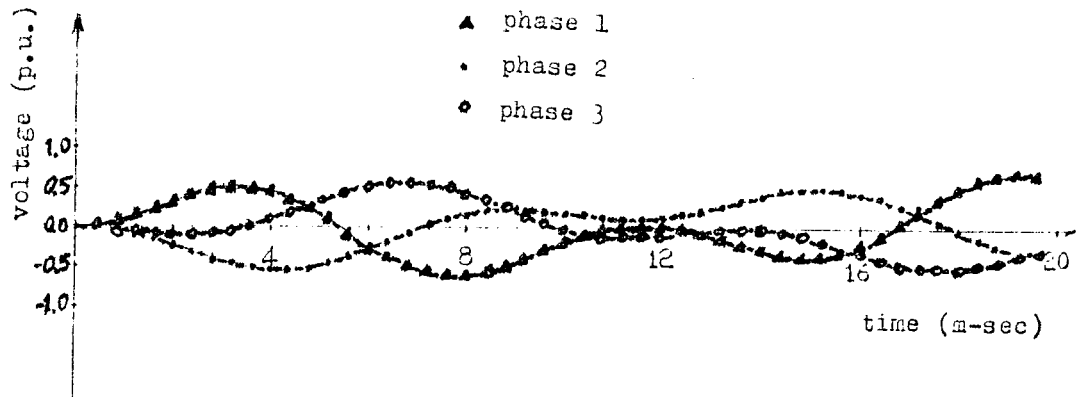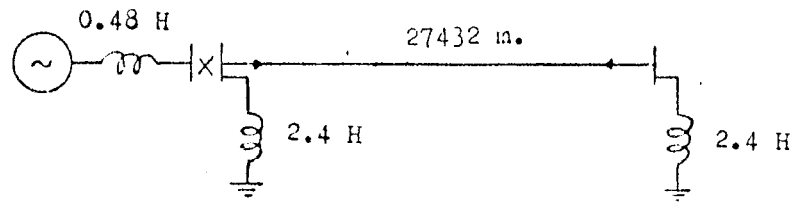
(a) Sending-end voltages
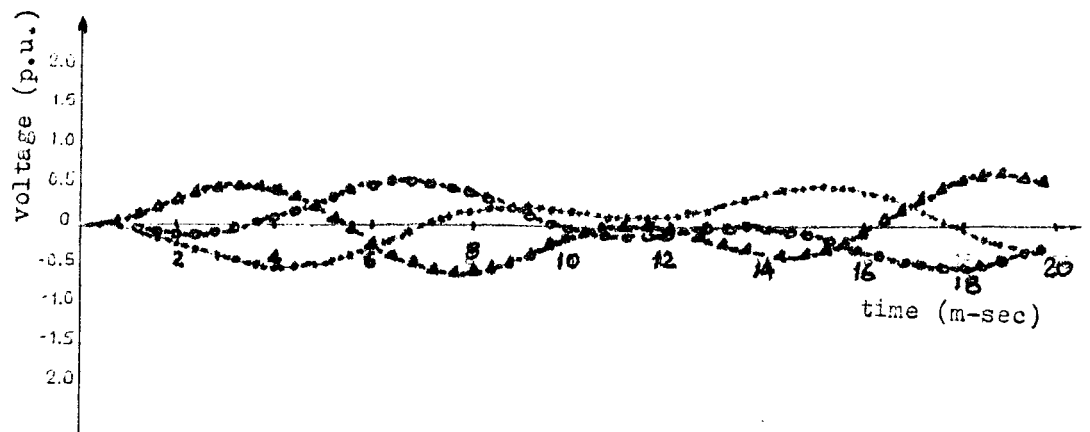
(b) Receiving-end voltages

Fig.4.13   Switching transients with 2.4 henry(100 MVar) shunt
compensation at both ends (source inductance=0.48 H)
NF_{max} = 50, NT_{max} = 100

62

Infinite
bus-bar ———|×|—————— 27432 m. —————|

▵ phase 1
. phase 2
○ phase 3

voltage (p.u.)

1.5
1.0
0.5
0.0
-0.5
-1.0
-1.5

2   4   6   8   10   12   14   16   18

time (m-sec)

(a) Sending-end voltages

voltage (p.u.)

2.0
1.5
1.0
0.5
0.0
-0.5
-1.0
-1.5
-2.0

2   4   6   8   10   12   14   16   20

time (m-sec)

(b) Receiving-end voltages
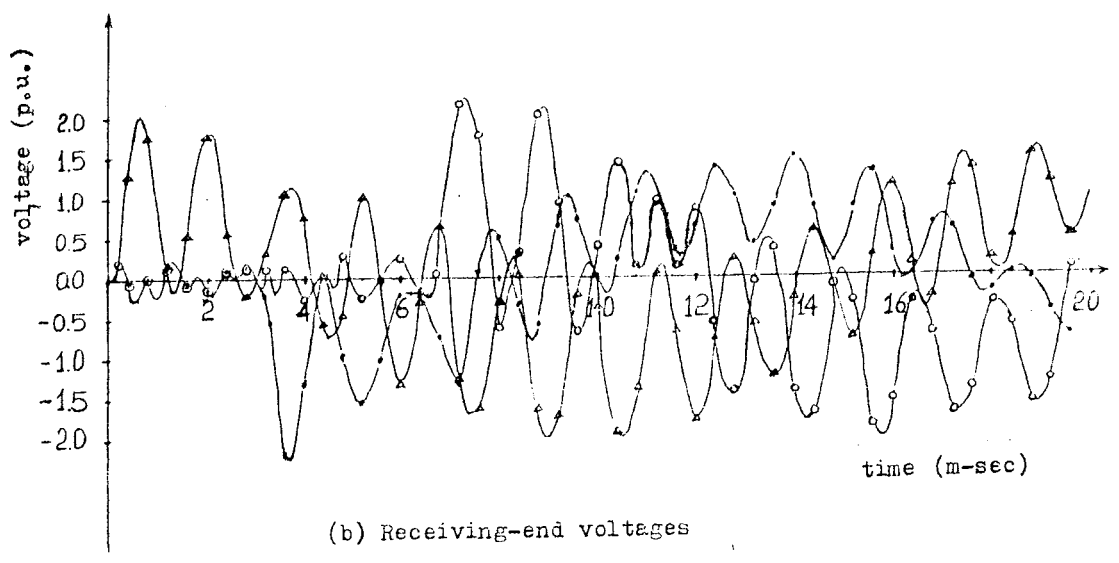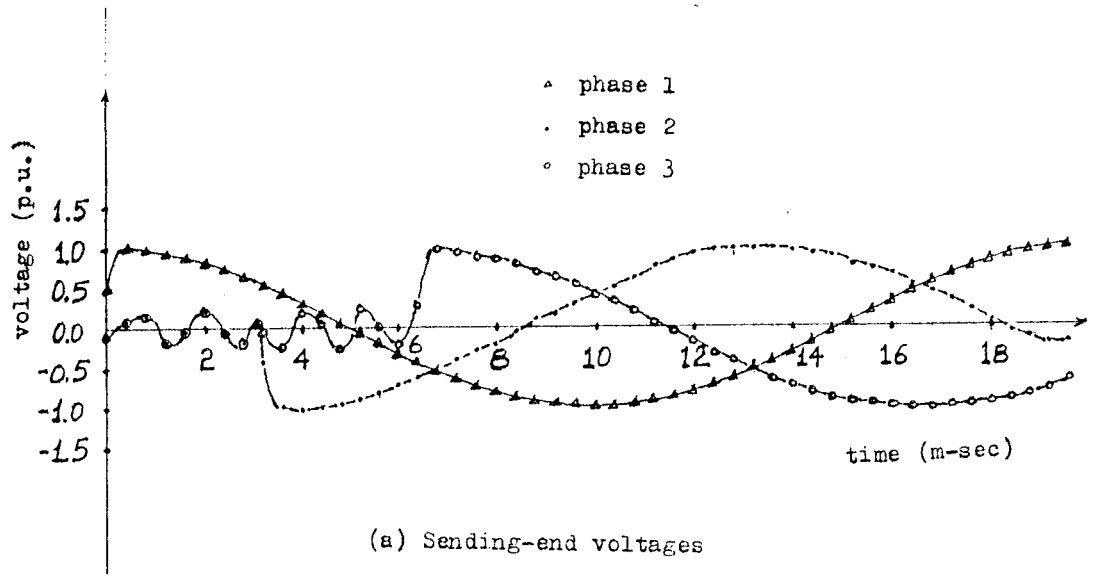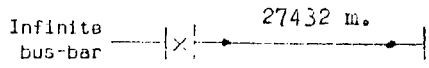
Fig.4.14   Switching transients with sequential pole closure,
           time delays are 3.2 and 6.6 ms.

$NF_{max} = 150$, $NT_{max} = 200$

Infinite bus-bar ⊢×⊦→ 27432 m.

△ phase 1
• phase 2
o phase 3

voltage (p.u.)

(a) Sending-end voltages

voltage (p.u.)

time (m-sec)
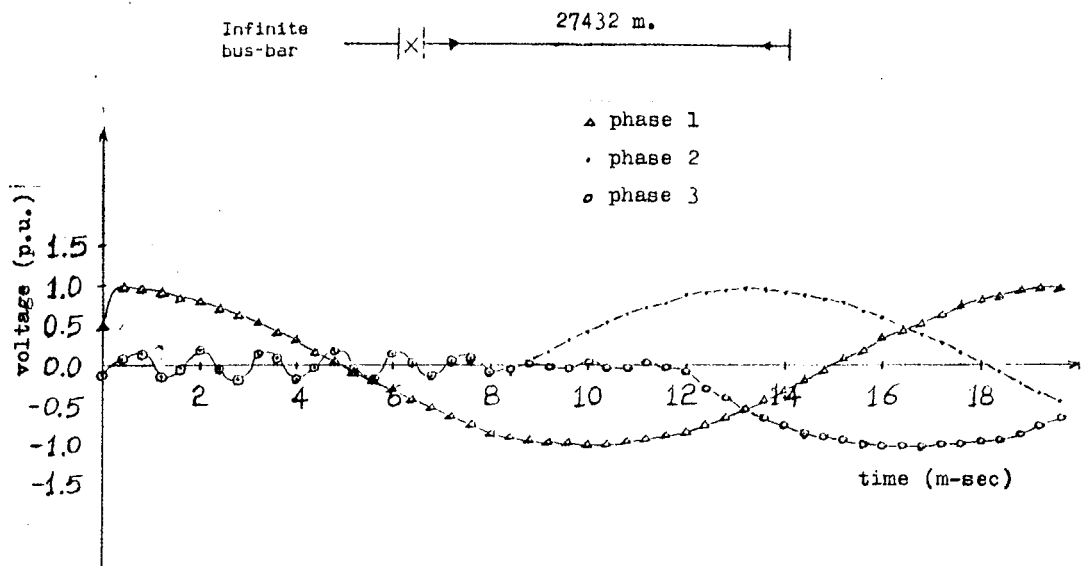
(b) Receiving-end voltages

Fig.4.15 Switching transient with sequential pole closure,
time delays are 8.4 and 11.6 ms
NF_{max} =150, NT_{max} = 200

64

CHAPTER 5

CONCLUSIONS

Throughout this work switching overvoltages in underground power cables are dealt with by the use of the modified Fourier transform method in conjuction with modal theory. Cable parameters are highly frequency dependent. By the choice of Fourier transform method frequency dependence of the cable parameters, skin effect, and earth-return path can be easily taken into account. The accuracy in the transient voltages is achieved by the proper choice of truncation frequency and the time step length.

A digitial computer program is developed by the author to handle the sequential pole closure problem as well as the simultaneous energisation in the switching overvoltage calculations.

Computer results show that; cable length, source impedance, shunt compensation and sequential pole closure angle affect the maximum magnitude of the switching overvoltages. Maximum receiving-end voltage magnitude increases with the cable length. Source impedance has a considerably high effect on the shape and magnitude of the transient voltage. As the source inductance increases, both the receiving-end and sending-end maximum voltage magnitudes increase. To minimize the adverse effect of the source impedance on the transient voltages, shunt reactor compensation can be used either at the sending-end or at both sending and receiving ends. When the dominant frequency of the system approaches the supply frequency shunt compensation is found to be effective to minimize the overvoltages.

In the case of sequential pole closure, nonlinear problem arises due to the change of system matrices with time. This nonlinear problem is solved using the piecewise Fourier transform method.

Sequential switching overvoltages are slightly higher than the simultaneous switching transients at receiving ends in the case of all the pole closures take place at their peak values. However, if the phase voltages across the breaker contacts are zero at the instant of closing breaker poles, transient overvoltages are considerably reduced.

Computation time in the modified Fourier transform method is long due to the eigenvalue and eigenvector calculations for a wide range of frequencies. If there is symmetry within the system conductors, the computation time is considerably saved making use of the symmetry conditions. Computation time, also, depends on the number of the frequency harmonics and time steps used in the calculation of the voltage responses. For 150 frequency harmonics and 200 time steps, execution time is 115 seconds in three-phase simultaneous energisation and 240 seconds in three-phase sequential energisation. If the number of frequency harmonics and time steps are chosen as 50 and 100, respectively, execution time becomes 38 seconds in three-phase simultaneous energisation.

In this study, sheath-bonding resistance of the crossbonded cable system is assumed to be zero and three-phase sequential energisation is from an infinite busbar. Transient analysis of the crossbonded cable system with the sheath-earthing resistance and sequential energisation from an inductive source may be the subject of future studies.

LIST OF REFERENCES

1- BICKFORD, J.P., and MULLINEUX, N., " Computation of Power System Transients " IEE Monograph Series 18, 1976.

2- BICKFORD, J.P. and DOEPEL, P.C., " Calculations of Switching Transients with Particular Reference to Line Energisation " IEE, Vol. 114, No.4, 1967

3- ADAMSON, C., Taha and WEDEPOHL, L.M., " Comparative Steady - state Performance of Crossbonded Cable System " IEE, Vol.115, No.8, 1968

4- WEDEPOHL, L.M. and WILCOX, D.J., " Transient Analysis of Underground Power - Transmission System " IEE, Vol. 120, No.2, 1973

5- WEDEPOHL, L.M., and INDULKAR, C.S., " Switching Overvoltages in Short Crossbonded Cable Systems using the Fourier Transform " IEE, Vol.122, No.11, 1975

6- DANG, N.D., " Transient Performance of Crossbonded Cable Systems " Ph.D. Thesis, University of Manchester Institute of Science and Technology, 1972

7- INDULKAR, C.S., " Wave Propagation in Multiconductor Crossbonded Cable Systems " Ph.D. Thesis, University of Manchester Institute of Science and Technology, 1970

8- WILCOX, D.J., and LOWLER, K.J., " Transient Phenomena in Crossbonded Cable Sytems : Analytical Results " IEE, Vol.125, No.10, 1978

9-   WEDEPOHL, L.M., and INDULKAR, C.S., " Switching
     Overvoltages in Long Crossbonded Cable Systems
     Using the Fourier Transform " IEEE, Vol.PAS - 98,
     No.4, 1979

10- NAGAOKA, N, AMETANI, A., " Transient Calculation on
     Crossbonded Cables " IEEE, Vol.PAS - 102, No.4,
     1983

11- ÜNVER, U., " Transient Analysis of Cable Systems
     Including the Effects of Nonlinear Protective
     Devices " Ph.D.Thesis, University of Manchester
     Institute of Science and Technology, 1979.

12- WEDEPOHL L.M., and MOHAMED S.E.T., " Transient
     Analysis of Multiconductor Transmission Lines with
     Special Reference to Nonlinear Problems "
     IEE, Vol.117, No.5, 1970.

13- LUCAS, J.R, " Crossbonded Cables and Analysis of
     Nonlinearities " M.Sc. Thesis, University of
     Manchester Institute of Science and Technology, 1972.

APPENDIX A

SERIES IMPEDANCE AND SHUNT ADMITTANCE MATRICES

A.1 Basic Cable Parameters

The cable consists of an inner conductor, conductor insulation, sheath, and sheath insulation as shown in Fig.A.1
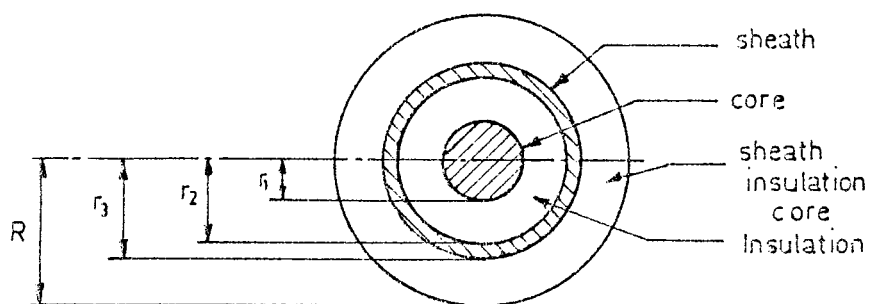
Fig.A.1 Cross-section of the one-core cable

ρ_1	Resistivity of inner conductor,
ρ_2	Resistivity of sheath,
ρ_e	Resistivity of earth return path,
ϵ_1	Permittivity of conductor dielectric,
ϵ_2	Permittivity of sheath dielectric.

A.2 Series Impedance

The exact solution for the series impedance com - ponents are obtained by using Bessel functions, since conducting paths depend on the frequency. However, simplified solutions are available which are applicable over a wide range of frequencies. [13]

(i) The internal impedance of the conductor is quite

accurately given by the expression

$$Z_c = \frac{\rho_1 m}{2\pi r_1} \cdot \text{Coth}\ (0.777\ m\ r_1) + \frac{0.356\ \rho_1}{\pi r_1^2}$$

where $m = (j\ w\mu/\rho_1)^{\frac{1}{2}}$

In particular, for very high frequency, where $w\mu/\rho_1 \gg 1$ the above formula reduces to the familiar skin effect formula $Z_c = \rho_1\ m/2\pi r_1$, and at very low frequency (or for d.c.) at which $w\mu/\rho_1 \ll 1$, the above gives the standard expression $Z_c = \rho_1/\pi r_1^2$.

(ii) The magnetic flux in the conductor dielectric gives rise to the conductor-sheath mutual impedance, which is given by the expression

$$Z_{sc} = \frac{j\ w\ \mu}{2\pi} \cdot \log_e\ (r_2\ /\ r_1)$$

(iii) The inner surface sheath impedance is approximately given by the expression

$$Z_{si} = \frac{\rho_2\ m}{2\pi r_2} \cdot \text{Coth}\ \left[m\ (r_3 - r_2) \right] - \frac{\rho_2}{2\pi r_2(r_3+r_2)}$$

where $m = (j\ w\mu/\rho_2)^{\frac{1}{2}}$

(iv) Due to the current flow in the sheath, a voltage is induced in the sheath-earth path giving rise to the mutual impedance between inner and **outer** sheath surfaces. This impedance is given by the expression

$$Z_m = \frac{\rho_2 \, m}{\pi(r_2 + r_3)} \, \text{Cosech} \left[m(r_3 - r_2) \right]$$

(v) The outer surface sheath impedance is given by the approximate expression

$$Z_{so} = \frac{\rho_2 \, m}{2\pi r_3} \cdot \text{Coth} \left[m(r_3 - r_2) \right] + \frac{\rho_2}{2\pi r_3 \, (r_3 + r_2)}$$

(vi) The flux in the sheath dielectric causes a mutual impedance between the sheath and earth and is given by the formula

$$Z_{se} = \frac{j \, w \, \mu}{2\pi} \cdot \log_e (R/r_3)$$

(vii) The earth return path has an impedance which may be represented by the following

$$Z_e = \frac{j \, w \, \mu_0}{2\pi} \cdot \left[6.4905 - \log_e p + k \, q - j(\frac{1}{4}\pi - k \, q) \right]$$

72

where $\quad q \quad = \quad (f/\rho_e)^{\frac{1}{2}}$

$\quad\quad\quad\quad f \quad = \quad$ frequency (Hz)

$\quad\quad\quad\quad p \quad = \quad q\,d$

$\quad\quad\quad\quad d \quad = \quad$ distance between cables

$\quad\quad\quad\quad k \quad = \quad 0.0013245\ (\ b + c\ )$

$\quad\quad\quad\quad b \quad = \quad$ depth of inducing cable $(b < 0)$

$\quad\quad\quad\quad c \quad = \quad$ depth of induced cable $(c < 0)$
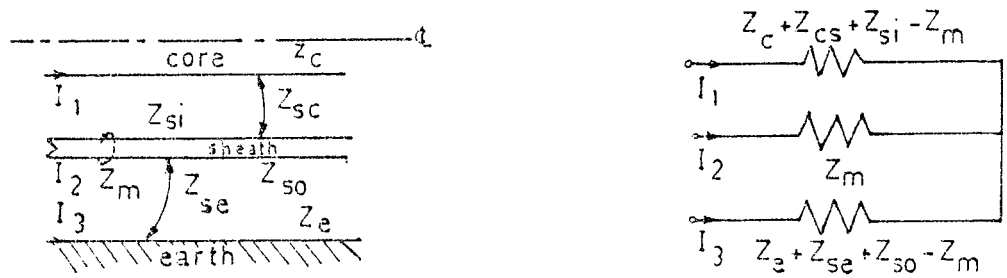
Fig. A.2 Cable impedances and equivalent circuit.

If the earth is taken as reference, the series impedance per unit length is given by the matrix

$$Z \quad = \quad \begin{array}{c} \\ c \\ \\ s \end{array} \overset{\begin{array}{cc} c & \quad\quad s \end{array}}{\begin{bmatrix} Z_{11} & Z_{12} \\ \\ Z_{12} & Z_{22} \end{bmatrix}}$$

where $\quad Z_{11} = Z_c + Z_{sc} + Z_{so} + Z_{se} + Z_e - 2\,Z_m$

$\quad\quad\quad\quad Z_{12} = Z_{so} + Z_{se} - Z_m$

$\quad\quad\quad\quad Z_{22} = Z_{so} + Z_{se} + Z_e$

73

A.3 Shunt Admittance

Evaluation of the shunt admittance matrix is quite straight forward. The three conducting paths form equipotential surfaces and may be represented as shown below.
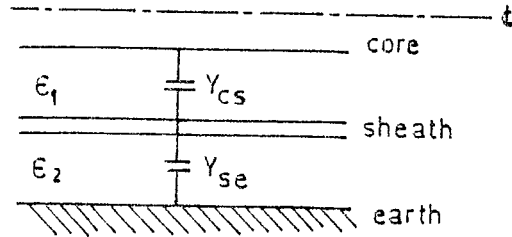
Fig.A.3 Component admittances of the cable.

If the dielectric loss is neglected, then the conductor-sheath and sheath-earth shunt admittances are readily given by the expressions

$$Y_{cs} = \frac{j w 2 \pi \epsilon_1}{\log_e (r_2/r_1)}$$

$$Y_{se} = \frac{j w 2 \pi \epsilon_2}{\log_e (R/r_3)}$$

If again, the earth is taken as reference, the shunt admittance matrix per unit length is given by

$$Y = \begin{array}{c} \\ c \\ s \end{array} \begin{array}{cc} c & s \\ \left[\begin{array}{cc} Y_{cs} & - Y_{cs} \\ -Y_{cs} & Y_{cs} + Y_{se} \end{array} \right] \end{array}$$

A.4 Mutual Impedance Between Adjacent Cables

As the earth return path may be considered as an electrostatic screen, there is no mutual admittance between adjacent cables. But due to the magnetic flux, there is substantial mutual impedance, which is highly dependent on frequency. The calculation is extremely complex, but suitable approximate formulas are available.

In general, the mutual impedance between cores, between sheaths, and between corresponding cores and sheaths are all equal. Their values are always less than the corresponding values of the earth return impedance.

For a three cable system, they take the following block form

a   b   c
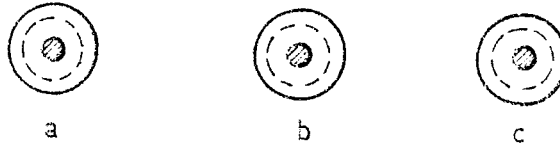
$$
Y = \begin{bmatrix}
Y_{cs} & -Y_{cs} & 0 & 0 & 0 & 0 \\
-Y_{cs} & Y_{cs}+Y_{se} & 0 & 0 & 0 & 0 \\
0 & 0 & Y_{cs} & -Y_{cs} & 0 & 0 \\
0 & 0 & -Y_{cs} & Y_{cs}+Y_{se} & 0 & 0 \\
0 & 0 & 0 & 0 & Y_{cs} & -Y_{cs} \\
0 & 0 & 0 & 0 & -Y_{cs} & Y_{cs}+Y_{se}
\end{bmatrix}
$$

a   b   c

The corresponding impedance matrix has the form

$$
Z =
\begin{array}{c}
\\
c_1 \\
s_1 \\
c_2 \\
s_2 \\
c_3 \\
s_3
\end{array}
\begin{array}{cccccc}
c_1 & s_1 & c_2 & s_2 & c_3 & s_3 \\
\left[\begin{array}{cccccc}
z_{11} & z_{12} & z_{13} & z_{13} & z_{15} & z_{15} \\
z_{12} & z_{22} & z_{13} & z_{13} & z_{15} & z_{15} \\
z_{13} & z_{13} & z_{11} & z_{12} & z_{15} & z_{15} \\
z_{13} & z_{13} & z_{12} & z_{22} & z_{15} & z_{15} \\
z_{15} & z_{15} & z_{15} & z_{15} & z_{11} & z_{12} \\
z_{15} & z_{15} & z_{15} & z_{15} & z_{12} & z_{22}
\end{array}\right]
\end{array}
$$

APPENDIX B

REDUCTION OF SYSTEM MATRICES

Series impedance and shunt admittance matrices may be reduced taking the sheath earthing conditions into account.

B.1 Sheathes Earthed Through Resistors

When the sheaths are solidly interconnected and earthed through resistors at both ends of the major section, terminal voltages of the three sheaths become equal. Hence the sheaths may be represented by an equivalent sheath. The equivalent sheath has the same voltage with the actual sheaths, but has a current equal to the sum of the three sheath currents. Hence the order of series impedence and shunt admittance matrices of the major section is reduced from 6x6 to 4x4.

The reduced matrices Y and Z have the following form.

$$
Y = \begin{array}{c} C_1 \\ C_2 \\ C_3 \\ S \end{array}
\begin{array}{cccc} C_1 & C_2 & C_2 & S \end{array}
\left[
\begin{array}{cccc}
Y_{cc} & 0 & 0 & -Y_{cs} \\
0 & Y_{cc} & 0 & -Y_{cs} \\
0 & 0 & Y_{cc} & -Y_{cs} \\
-Y_{cs} & -Y_{cs} & -Y_{cs} & 3Y_{ss}
\end{array}
\right]
$$

and

$$Z = \begin{array}{c} \\ C_1 \\ C_2 \\ C_3 \\ S \end{array} \overset{\begin{array}{cccc} C_1 & \quad C_2 & \quad C_3 & \quad S \end{array}}{\begin{bmatrix} z_{11} & z_{12} & z_{12} & z_{14} \\ z_{12} & z_{11} & z_{12} & z_{14} \\ z_{12} & z_{12} & z_{11} & z_{14} \\ z_{14} & z_{14} & z_{14} & z_{44}^{*} \end{bmatrix}}$$

where $Y_{ss} = Y_{cs} + Y_{se}$

$$z_{44}^{*} = (z_{44} + 2z_{12}) / 3$$

Admittances and impedances shown above are mentioned in Appendix A.

B.2 Sheaths Solidly Earthed

When the sheath earthing resistances are assumed to be zero, a possible simplification can also be introduced by eliminating the rows and columns corresponding to the sheath in the series impedance and shunt admittance matrices to eliminate the rows and columns corresponding to the sheaths from the admittance matrices, boundary conditions are employed, so that reduced equivalent admittance matrices can be obtained. However, to eliminate sheaths from the impedance matrices, first the rows and columns corresponding to the sheaths are removed from the inverted impedance matrix and then the reduced matrix is re-inverted. After the elimination of sheaths from the series impedance matrix of a cable, given in Appendix A, the reduced impedance matrix may be given as

$$Z_R = Z_c - Z_{sc} \, Z_{ss}^{-1} \, Z_{sc}^T$$

Using this equation the impedance elements corresponding to the sheaths must be placed at the extreme rows and columns in the original impedance matrix. In this case impedance matrix is given by,

$$Z = \begin{array}{c} c_1 \\ c_2 \\ c_3 \end{array} \left[\begin{array}{ccc} z_{11}' & z_{12}' & z_{12}' \\ z_{12}' & z_{11}' & z_{12}' \\ z_{12}' & z_{12}' & z_{11}' \end{array} \right]$$

where
$$z_{11}' = z_{11} - z_{14}^2 / z_{44}^*$$

$$z_{12}' = z_{12} - z_{14}^2 / z_{44}^*$$

the admittance matrix is also reduced to give

$$Y = \begin{array}{c} c_1 \\ c_2 \\ c_3 \end{array} \left[\begin{array}{ccc} Y_{cs} & 0 & 0 \\ 0 & Y_{cs} & 0 \\ 0 & 0 & Y_{cs} \end{array} \right]$$

In this case, the product matrix $P = ZY$ is given by

$$P = Y_{cs} \left[\begin{array}{ccc} z_{11}' & z_{12}' & z_{12}' \\ z_{12}' & z_{11}' & z_{12}' \\ z_{12}' & z_{12}' & z_{11}' \end{array} \right]$$

APPENDIX C

DETERMINATION OF EIGENVALUES AND

EIGENVECTORS OF SYMMETRICAL CROSS-BONDED CABLE SYSTEMS

In the system studied, it is necessary to determine eigenvalues and eigenvectors of the matrix product ZY, where Z and Y are series impedance and shunt admittance matrices, respectively. The eigenvalues of the matrix $P = ZY$ can be obtained being the roots of the characteristic equation,

$$\det (P - \lambda U) = 0$$

where U is the unit matrix having the same order as P. If P is a matrix of order n, then this determinant yields an nth order polynomial in which are the eigenvalues of P. The eigenvector Q_i corresponding to the eigenvalue λ_i can be evaluated from

$$(P - \lambda_i U) Q_i = 0$$

The eigenvectors, thus found, form eigenvector matrix Q of order $n \times n$.

The orders of series impedance and shunt admittance matrices depend on the sheath earthing conditions as shown in Appendix B. Therefore, when evaluating the eigenvectors of the cross-bonded cable systems, sheath earthing conditions should be taken into account.

C.1 Factorization Method for Systems with Odd Symmetry [11]

In systems with odd symmetry, there exists an odd number of conductors, such that the odd conductor lies on a reference plane perpendicular to the ground plane and the other conductors are arranged in pairs at the same vertical distances from the ground and at equal horizontal distances on either side of the reference plane. Flat and trefoil arrangements of single- circuit cable systems, for example, are systems having odd symmetry among their conductors. For such a system, the matrix P takes the general form

$$P = \begin{bmatrix} P_a & P_b & P_c \\ P_b & P_a & P_c \\ P_d & P_d & P_e \end{bmatrix}$$

where P_a and P_b are square matrices of order $(n-m)/2$, n being the order of P matrix and m being the number of odd conductors lying on the reference plane; P_c is a column matrix of order $(n-m)/2 \times m$; P_d is a row matrix of order $m \times (n-m)/2$, and P_e is of order $m \times m$.

Transformation matrices K and K^{-1} will be introduced so that

$$K^{-1} \; PK = P_1 = \begin{bmatrix} P_a - P_b & & 0 \\ 0 & P_a + P_b & P_c \\ 0 & 2P_d & P_e \end{bmatrix}$$

The matrices K and K^{-1} may be given as

$$K = \begin{bmatrix} U_1 & U_1 & 0 \\ -U_1 & U_1 & 0 \\ 0 & 0 & U_2 \end{bmatrix} \; ; \quad K^{-1} = \frac{1}{2} \begin{bmatrix} U_1 & -U_1 & 0 \\ U_1 & U_1 & 0 \\ 0 & 0 & 2U_2 \end{bmatrix}$$

where U_1 and U_2 are unit matrices of orders $(n-m)/2$ and m, respectively. The matrices P and P_1 have the same eigenvalues, and hence

$$\det(P - \lambda U) = \det(P_1 - \lambda U) = \det\left(K^{-1}(P - \lambda U)K\right)$$

The equation may be written as

$$\det(P_1 - \lambda U) = \det \begin{bmatrix} P_a - P_b - \lambda U_1 & 0 & 0 \\ 0 & P_a + P_b - \lambda U_1 & P_c \\ 0 & 2P_d & P_e - \lambda U_2 \end{bmatrix}$$

$$= \det(P_a - P_b - \lambda U_1) \cdot \det \begin{bmatrix} P_a + P_b - \lambda U_1 & P_c \\ 2P_d & P_e - \lambda U_2 \end{bmatrix}$$

From the theory of matrix functions, the following equation can be written

$$\det(P_a - P_b - \lambda U_1) = 0$$

$$\det \begin{bmatrix} P_a + P_b - \lambda U_1 & P_c \\ 2P_d & P_e - \lambda U_2 \end{bmatrix} = 0$$

Thus, the solution of an nth order polynomial has been reduced to the solutions of two polynomials, each having orders of $(n-m)/2$. The eigenvalues of these equations can be evaluated using root-squaring method.

82

The eigenvector matrix of P_1 is of the form

$$Q' = \begin{bmatrix} Q'_a & 0 \\ 0 & Q'_b \\ 0 & Q'_c \end{bmatrix}$$

where Q'_a, Q'_b and Q'_c are eigenvector submatrices having orders of $(n-m)/2$, $(n-m)/2$ and m, respectively. The eigenvector matrix of P can be readily given as

$$Q = KQ' = \begin{bmatrix} U_1 & U_1 & 0 \\ -U_1 & U_1 & 0 \\ 0 & 0 & U_2 \end{bmatrix} \begin{bmatrix} Q'_a & 0 \\ 0 & Q'_b \\ 0 & Q'_c \end{bmatrix}$$

or

$$Q = \begin{bmatrix} Q'_a & Q'_b \\ -Q'_a & Q'_b \\ 0 & Q'_c \end{bmatrix}$$

C.2 Sheaths Earthed Through Resistors

When the sheaths are solidly interconnected and earthed through resistors at the major section terminations, the order of the P matrix is reduced, and may be expressed as

$$P = Z\,Y = \begin{bmatrix} P_{11} & P_{12} & P_{12} & P_{14} \\ P_{12} & P_{11} & P_{12} & P_{14} \\ P_{12} & P_{12} & P_{11} & P_{14} \\ P_{41} & P_{41} & P_{41} & P_{44} \end{bmatrix}$$

Defining the transformation matrix K and its inverse K^{-1} as

$$K = \begin{bmatrix} 1 & -\frac{1}{2} & 1 & 0 \\ 0 & 1 & 1 & 0 \\ -1 & -\frac{1}{2} & 1 & 0 \\ 0 & 0 & 0 & 1 \end{bmatrix}, \text{ and } K^{-1} = \begin{bmatrix} \frac{1}{2} & 0 & -\frac{1}{2} & 0 \\ -\frac{1}{3} & \frac{2}{3} & -\frac{1}{3} & 0 \\ \frac{1}{3} & \frac{1}{3} & \frac{1}{3} & 0 \\ 0 & 0 & 0 & 1 \end{bmatrix}$$

$P_1 = K^{-1}\,P\,K$ is defined, [13] and has block diagonal form, i.e.

$$P_1 = \begin{bmatrix} P_{11} {}^{-}P_{12} & 0 & 0 & 0 \\ 0 & P_{11} {}^{-}P_{12} & 0 & 0 \\ 0 & 0 & P_{11} {}^{+}P_{12} & P_{14} \\ 0 & 0 & 3\,P_{41} & P_{44} \end{bmatrix}$$

84

which gives the eigen values directly as

$$\lambda_1 = \lambda_2 = P_{11} - P_{12}$$

and the remaining 2 values being those of the (2x2) matrix

$$\begin{bmatrix} P_{11} + 2 P_{12} & P_{14} \\ 3 P_{41} & P_{44} \end{bmatrix}$$

The modal matrix of P_1 will have the form

$$Q_1 = \begin{bmatrix} 1 & 0 & 0 & 0 \\ 0 & 1 & 0 & 0 \\ 0 & 0 & 1 & 1 \\ 0 & 0 & x & y \end{bmatrix}$$

where

$$x = \frac{-3 P_{41}}{P_{44} - \lambda_3}, \quad \text{and} \quad y = \frac{-(P_{11} + 2P_{12} - \lambda_4)}{P_{14}}$$

Now the modal matrix of the original matrix is obtained from

$$Q = \begin{bmatrix} 1 & -\frac{1}{2} & 1 & 1 \\ 0 & 1 & 1 & 1 \\ -1 & -\frac{1}{2} & 1 & 1 \\ 0 & 0 & x & y \end{bmatrix}$$

85

and its inverse is given by

$$Q^{-1} = \begin{bmatrix} \dfrac{1}{2} & 0 & -\dfrac{1}{2} & 0 \\[2ex] -\dfrac{1}{3} & \dfrac{2}{3} & -\dfrac{1}{3} & 0 \\[2ex] \dfrac{y}{3(y-x)} & \dfrac{y}{3(y-x)} & \dfrac{y}{3(y-x)} & \dfrac{-1}{(y-x)} \\[2ex] \dfrac{-x}{3(y-x)} & \dfrac{-x}{3(y-x)} & \dfrac{-x}{3(y-x)} & \dfrac{1}{(y-x)} \end{bmatrix}$$

C.3 Sheats Earthed Solidly

For this special case, the eigenvalues can be found by inspection. Thus the three associated propagation con- constants are evaluated from the equation

$$\det (P - k_i\, U) = 0$$

to give

$$k_1 = k_2 = Y_{cc}\,(Z_{11}' - Z_{12}')$$

and

$$k_3 = Y_{cc}\,(Z_{11}' + 2\,Z_{12}')$$

Y_{cc}, Z_{11}', and Z_{12}' are given in Appendix B.

Reduced impedance and admittance matrices have the orders 3x3. The modal matrix of $P = ZY$ and its inverse is given by

$$Q = \begin{bmatrix} 1 & -\dfrac{1}{2} & 1 \\[2ex] 0 & 1 & 1 \\[2ex] -1 & \dfrac{-1}{2} & 1 \end{bmatrix} \qquad Q^{-1} = \begin{bmatrix} -\dfrac{1}{2} & 0 & -\dfrac{1}{2} \\[2ex] -\dfrac{1}{3} & \dfrac{2}{3} & -\dfrac{1}{3} \\[2ex] \dfrac{1}{3} & \dfrac{1}{3} & \dfrac{1}{3} \end{bmatrix}$$

PIECEWISE FOURIER TRANSFORM OF IRREGULAR TIME FUNCTIONS

In sequential pole closure analysis, during the time interval between the first and second pole closure, a certain amount of energy transfer takes place between the energized conductor(s) of the system and the other floating conductor(s) , the coupled conductor(s) thus acquire voltages. These voltages are calculated numerically in time domain and to find their Fourier transforms, piecewice analysis is used [12] .

Consider an irregular time function $f(t)$ which is divided into K strips of width t_0 and $f(t)$ is assumed to vary linearly over such a strip, as shown in figure (D.1.a.)

The Fourier transform of the function bounded by the points $(n-1) t_0 \longrightarrow f_{n-1} \longrightarrow f_n \longrightarrow nt_0$ can be found if this is decomposed into a series of step and ramp functions whose transforms are readily obtained. Fig. (D.1.b.) gives a possible decomposition with two step and two ramp functions. The magnitudes of steps are f_{n-1} and $-f_n$ and the slopes of the ramps are $\Delta f_n / t_0$ and $- \Delta f_n / t_0$.

Fourier transform of the unit step function is

$$1 / (jw)$$

The transform contribution from all strips of $f(t)$ due to all steps is given by

87

$$F_1(w) = \frac{1}{jw} \left\{ f_o - f_N \left[\exp(-jNw\,t_o) \right] \right\}$$

where f_o is the value of $f(t)$ when $t = 0$ and f_N is the value of $f(t)$ at $t = N\,t_o$, N being the number of strips.
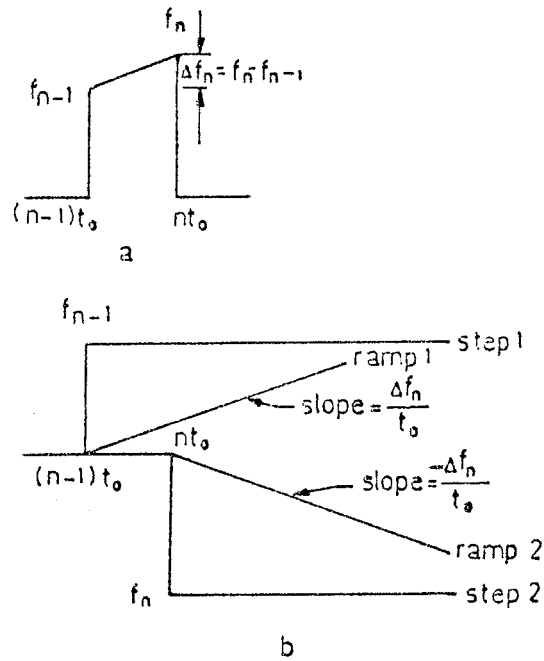

Fig. D.1 Composition of $f(t)$

a- Typical strip

b- Possible form of reduction

The transform of a ramp function with slope m is
$m / (jw)^2$, then the transform contribution of all ramps
can be written as ;

$$F_2(w) = - \frac{1}{w^2} \sum_{n=1}^{N} \frac{\Delta f_n}{t_o} \left\{ \exp \left[-j (n-1) w t_o \right] \right.$$

$$\left. - \exp (-j n w t_o) \right\}$$

the complete transform of $f(t)$ is

$$F(w) = F_1(w) + F_2(w)$$

Assuming the function starts and finishes at zero,
the transform of the irregular time function $f(t)$ will
have the form given below.

$$F(w) = - (1/w^2 t_o) \left\{ f_1 + f_{N-1} \left[\exp (-jNwt_o) \right] + \right.$$

$$\left. \sum_{n=1}^{N-1} (f_{n+1} - 2f_n + f_{n-1}) \left[\exp (-j n w t_o) \right] \right\}$$

In the calculation of power system transients due
to switching operations, a modified form of Fourier
transform is used, and this is accomplished by replacing
(w) with $(w-j \alpha)$.